Research Square

Preprints are preliminary reports that have not undergone peer review.
They should not be considered conclusive, used to inform clinical practice,
or referenced by the media as validated information.

Proteomic and Metabolomic Profiling and Functional Annotation of Two Drought-tolerant Tef [Eragrostis tef (Zucc.) Trotter] Genotypes During Dehydration and Rehydration

Beakal Tadesse Girma

grmbea001@myuct.ac.za

University of Cape Town https://orcid.org/0000-0002-0210-3455

Llewelyn Van Der Pas

University of Cape Town

Hawwa Gabier

University of Cape Town

Amsalu Gobena Roro

Hawassa University

Ali Elnaeim Elbasheir Ali

University of Mpumalanga

Kebebew Assefa Abebe

Ethiopian Institute of Agricultural Research

Abel Teshome

International Livestock Research Institute

Zerihun Tadele

University of Bern

Jill M. Farrant

University of Cape Town

Research Article

Keywords: Drought 1, Gene ontology 2, KEGG Pathway 3, Proteins 4, Metabolites 5 Tef 6

Posted Date: November 20th, 2026

DOI: https://doi.org/10.21203/rs.3.rs-11791081/v1

License: This work is licensed under a Creative Commons Attribution 4.0 International License.
Read Full License

Additional Declarations: The authors declare no competing interests.

Proteomic and Metabolomic Profiling and Functional Annotation of Two Drought-tolerant Tef [*Eragrostis tef* (Zucc.) Trotter] Genotypes During Dehydration and Rehydration

Beakal Tadesse Girma [1,2*], Llewelyn Van Der Pas[1], Hawwa Gabier[1], Amsalu Gobena Roro [3], Ali Elnaeim Elbasheir Ali[4], Kebebew Assefa Abebe[2], Abel Teshome[5], Zerihun Tadele[6,7] and Jill M. Farrant[1*]

[1] Department of Molecular and Cell Biology, University of Cape Town, Cape Town, South Africa
[2] Ethiopian Institute of Agricultural Research, Addis Ababa, Ethiopia
[3] Department of Plant and Horticultural Sciences, Hawassa University, Hawassa, Ethiopia
[4]School of Biology and Environmental Sciences, Faculty of Agriculture, Health and Natural Sciences, University of Mpumalanga, Mbombela, South Africa
[5]International Livestock Research Institute, Addis Ababa, Ethiopia
[6]Institute of Plant Sciences, University of Bern, Bern, Switzerland
[7]Department of Plant Sciences, Bahir Dar University, Bahir Dar, Ethiopia
[*] Correspondence: grmbea001@myuct.ac.za, jill.farrant@uct.ac.za

Abstract

This study aimed to identify proteomic, and metabolomic responses associated with dehydration and subsequent recovery in two drought-tolerant tef genotypes. At the end of drought, proteomic analysis revealed increased abundance of stress-protective proteins, regulating protein homeostasis and osmotic adjustment. Gene ontology analysis revealed enrichment of mRNA processing and alternative splicing pathways. Antioxidant responses differed between the two genotypes. RIL44 enriched glyoxal metabolic process whereas, Boni increased L-proline biosynthesis. Metabolomic analyses supported these findings, showing increased accumulation of proline and glutamic acid at the end of drought. KEGG pathway analysis during drought revealed downregulation of secondary metabolism, phenylpropanoid, and lignin pathways. Metabolomic data further showed increased accumulation of arabitol and meso-erythritol, sugar alcohols associated with osmotic regulation and cell wall modification. Recovery induced xyloglucan metabolic process, amino sugar and nucleotide sugar metabolism supporting cell growth and expansion. Moreover, methylation and vesicle budding were downregulated during recovery. RIL44 exhibited earlier downregulation of glucuronoxylan biosynthesis related with lower accumulation of secondary cell-wall and increased accumulation other metabolites at end the of drought, which may be related to its rapid morphophysiological recovery, whereas Boni showed a more gradual restoration. Overall, tef drought tolerance involves molecular chaperone induction, genotype-specific antioxidant strategies, metabolic reprogramming, and dynamic regulation of cell-wall biosynthesis. These findings highlight distinct molecular responses to dehydration and recovery in tef and may provide potential targets for breeding and biotechnological approaches aimed at improving drought resilience in tef and potentially other crops.

Keywords: Drought 1, Gene ontology 2, KEGG Pathway 3, Proteins 4, Metabolites 5 Tef 6

1 Introduction

Climate change is intensifying the frequency and severity of drought worldwide, threatening food security, particularly in Africa [1,2]. To sustain production under such stress, diversifying into orphan crops that tolerate adverse conditions is a key strategy [3]. Orphan cereals are often nutrient-dense and adapted to diverse environments including drought. *Eragrostis tef* (tef) is one such crop: a C4 cereal endemic to Ethiopia that is gluten-free and rich in minerals and proteins [4]. Tef is a staple grain crop in Ethiopia grown on ~3 million ha (~30% of arable land) and yielding ~5 million tonnes of grain to feed over 70 million people [5,6]. Both grain and straw are highly valued (often more than wheat or barley), reflecting tef's high nutritional quality and palatability [7].

Tef is remarkably adaptable: it grows across diverse agro-ecologies (1000–2500 m elevation) and tolerates drought, heat and waterlogging conditions better than most common cereals [7]. For example, tef plants can withstand ~50% leaf water loss (relative water content) before cell injury occurs [8]. Despite this resilience, severe or terminal drought can substantially reduce tef yield (e.g. 50-80% grain yield loss in extreme conditions) [9,10]. In Ethiopia, increasingly erratic rainfall patterns and recurrent drought represent a major constraints on tef production, reducing yield and potentially limiting arable land suitable for cultivation [11]. Improving drought tolerance in tef is therefore an important effort.

In addition to surviving drought stress, the ability of plants to recover after rewatering is an important aspect of drought resilience. Although some plants can tolerate severe water loss, drought can affect several physiological and metabolic processes, including photosynthesis, respiration and growth [12]. Once water becomes available again, plants need to restore their water balance, repair cellular damage and resume normal physiological and metabolic activities. However, the rate and extent of recovery can differ depending on the severity and duration of drought stress, as well as the plant genotype [13,14]. Studying plant responses during both drought and recovery can therefore provide a better understanding of the mechanisms involved in drought tolerance and the restoration of normal plant functions following rewatering.

Conventional breeding has released many improved tef varieties [7], but progress is slow for complex traits like drought tolerance (which is polygenic with high genotype×environment interaction effects) [15]. Traditional breeding approaches can be constrained by the time required to develop and evaluate new varieties, often struggling under challenges in response to rapidly changing climate conditions [13]. Multi-omics approaches provide a complementary strategy for investigating drought resilience. Integrating genomics, transcriptomics, proteomics, metabolomics and advanced phenotyping can identify key genes, proteins and metabolites underlying stress resilience [16–18]. Proteomics provides direct insight into changes in protein abundance and associated biological processes in response to drought, capturing information at the protein level not evident from gene expression alone [19]. Likewise, metabolomic profiling reveals changes in primary and secondary metabolites that bridge molecular responses and phenotypes. Together, temporal "downstream" profiling of proteins and metabolites under dehydration (and recovery) can identify biomarkers of tolerance and candidate genes for breeding [20,21].

Despite these opportunities, a comprehensive multi-omics investigation of drought response in tef is still lacking [8,22,23]. Most studies so far have focused primarily on the genomics of landraces and older varieties, while relatively few have investigated drought-induced changes at the protein and metabolite levels in tef genotypes. Indeed, only one study has applied proteomics to investigate drought stress responses in a

tef genotype [8]. Bridging this gap, we combined label-free proteomics and metabolomics to unravel drought resistance mechanism in improved tef genotypes.

This study aimed to elucidate the molecular mechanisms underlying drought tolerance in two tef genotypes, in which previous studies have shown contrasting drought tolerance responses. Here we identified differentially abundant proteins (DAPs) during drought and subsequent recovery. Proteomic findings were further supported by metabolomic analysis by examining differentially accumulated metabolites (DAMs). Functional annotation of DAPs and DAMs using Gene Ontology (GO) and Kyoto Encyclopedia of Genes and Genomes (KEGG) pathway analyses was performed to identify the biological processes and metabolic pathways associated with drought response and recovery.

2 Results

Two drought-tolerant tef genotypes, Boni and RIL44, were selected for this study based on their contrasting drought adaptation mechanisms identified in previous studies [24,25]. Figure 1 shows the change in morphology of both genotypes during hydration, dehydration and rehydration phases.

At the onset of dehydration, tef plants were green with no visible leaf rolling. As drought progressed, leaves became curly, rolled, pin-shaped phenotypes increased. By the end of the drought period, no green leaves were observed. During rehydration, leaf unfolding and the emergence of new green leaves were observed. This was more rapid in RIL44 occurring 2 days after rehydration. Boni, by comparison, showed no signs of recovery. After 10 days of rehydration, both genotypes had more newly emerging and unfolding leaves, along with the development of new tillers.

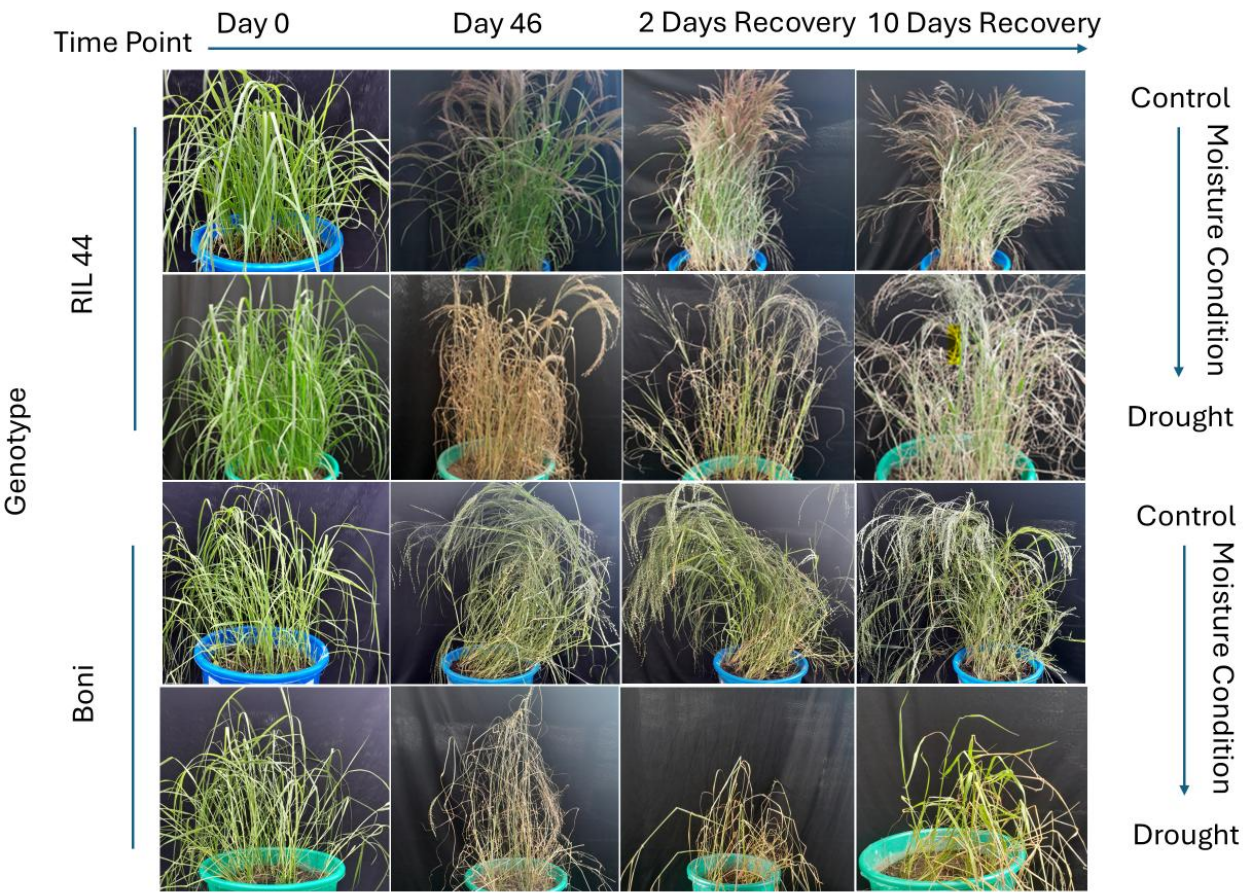


Figure 1 Two drought tolerant tef genotypes (Boni and RIL44) were subjected to drought stress and rehydration.

Note: Control plants remained fully hydrated (85-94% RWC) throughout the four time points (Day 0 and 46 after drought; 2 and 10 days of recovery). Drought stressed plants were at four time points as well: Day 0 (beginning of drought, 84-94% RWC), Day 46 (end of drought, 24-30% RWC), 2 days after rehydration (30-55% RWC) representing 2 days after recovery (early recovery) and 10 days after rehydration (76-85% RWC) representing 10 days after recovery (late recovery).

2.1 **Tef dehydration and rehydration treatment**

In Boni, at the onset of drought stress, the average soil gravimetric water content (GWC) was 40% (Supplementary Figure 2 and Table S1), while the leaf relative water content (RWC) ranged between 89% and 90% (Supplementary Table S2). In the fully hydrated control plants, both soil GWC and leaf RWC remained within these ranges across all sampling points, with no significant changes observed. In drought-stressed plants, however, 46 days without irrigation significantly reduced soil GWC to 5% and leaf RWC to an average of 24%. Following two days of rehydration, soil GWC recovered to 35%, while leaf RWC showed only a slight increase to 29%. After 10 days of recovery, soil GWC reached 39% and leaf RWC improved substantially to 85%.

In RIL44, the soil and leaf water content in the fully hydrated control plants remained between 40-41% and 85-94%, respectively. In drought-stressed plants, soil GWC significantly declined from 38% at the onset of drought to 6% after 46 days without irrigation. Then it recovered to 38% and 35% after 2 and 10 days of rehydration, respectively. Leaf RWC significantly decreased from 92% at the beginning of drought to 31% after 46 days of dehydration. Then, subsequently increased to 52% and 77% after 2 and 10 days of recovery, respectively.

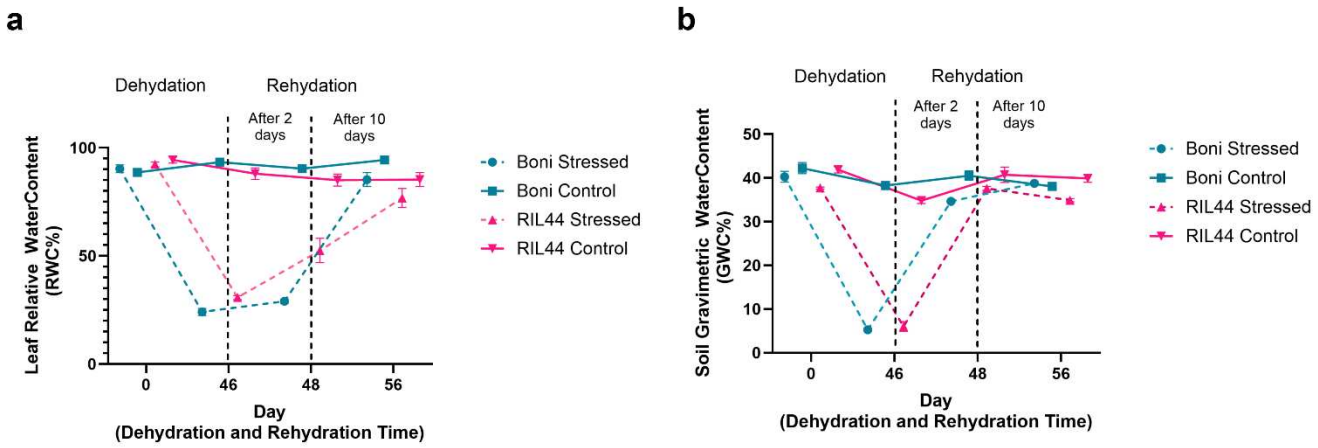


*Figure 2 Change in soil and leaf water content of two drought tolerant tef genotypes (Boni and RIL44) subjected to drought stress and rehydration with their respective control. (**a**) Change in the soil gravimetric water content (GWC); and (**b**) Leaf relative water content (RWC).*

2.2 Separate analysis for individual groups

Differential protein and metabolite analyses were performed across 16 treatments encompassing two genotypes, two moisture conditions, and four sampling points. The treatments were organized into six pairwise comparisons for the two drought-tolerant tef genotypes, Boni and RIL44. The comparisons are designated as follows:

1. **Growth:** The comparison between the fully hydrated control on day 46 after drought (ContD46) and the fully hydrated control at the beginning of drought (ContD0). This comparison was conducted to investigate biochemical changes and their biological implications in regularly watered non stressed tef plants.

2. **End of drought:** The comparison between drought-stressed plants on day 46 after drought (StrD46) and the fully hydrated control at the end of drought (ContD46).

3. **Early recovery I:** The comparison between drought-stressed plants after 2 days of rehydration (StrR2) and the fully hydrated control at the end of drought (ContD46).

4. **Late recovery I:** The comparison between drought-stressed plants after 10 days of rehydration (StrR10) and the fully hydrated control at the end of drought (ContD46).

5. **Early recovery II:** The comparison between drought-stressed plants after 2 days of rehydration (StrR2) and the fully hydrated control after 2 days of rehydration (ContR2).

6. **Late recovery II:** The comparison between drought-stressed plants after 10 days of rehydration (StrR10) and the fully hydrated control after 10 days of rehydration (ContR10).

2.3 Differentially abundant analysis of proteins for two drought tolerant tef genotypes during growth, end of drought and recovery

A total of 7319 non-redundant proteins were identified in this study from 16 treatments comprising two genotypes, two moisture conditions, and four sampling points. After filtering, imputation, and normalization, 4310 proteins remained. Subsequently, two way ANOVA identified 3810 significantly different proteins.

The R based MetaboAnalyst 6.0 platform was used to calculate differentially abundant analysis of proteins in different conditions. The DAPs were identified based on $log_2FC \pm 1$, p value (<0.05) and Bonferroni corrected for FDR <0.05. This was supplemented by the Uniprot accession no., their description and GO term ID for DAPs (Additional Table1) is available at

https://figshare.com/s/6e7dfb7f35c58ae1261e.

After ANOVA, a total of 3810 non-redundant proteins were identified across all treatments. Table 1 shows the number of DAPs across different genotypes and conditions. The highest number of DAPs were shown during growth (804) and during early recover I (755). The lowest number of DAPs were shown during late recovery II (183).

Boni exhibited the highest number of DAPs during early recovery and the lowest during late recovery. In contrast, RIL44 showed the highest number of DAPs during the growth and the lowest (zero) during early recovery. Overall, RIL44 displayed fewer DAPs than Boni throughout the recovery periods and the remaining conditions.

Table 1 Number of differentially abundant proteins (DAPs) that are unique and shared between the drought tolerant tef genotypes Boni and RIL44 during growth, end of drought, and recovery stages.

Conditions	Boni		RIL44		Common	
	Increased	Decreased	Increased	Decreased	Increased	Decreased
Growth	128	146	135	157	142	96
End of Drought	255	247	23	24	95	103
Early Recovery I	363	391	0	0	1	0
Late Recovery I	140	117	0	0	0	0
Early Recovery II	291	323	1	0	5	3
Late Recovery II	59	57	6	21	17	23

Note: Conditions represent DAPs with paired treatment comparisons representing growth: ContD46/ ContD0, end of drought: StrD46/ ContD46, early recovery I: StrR2/ContD46, late recovery I: StrR10/ContD46, early recovery II: StrR2/ContR2, and late recovery II: StrR10/ContR10. Where: Cont: control, Str: drought stressed, D0 and D46: 0 and 46 days after dehydration; R2 and 10: 2 and 10 days after rehydration.

2.4 **Gene ontology (GO) annotation for differentially abundant proteins (DAPs) during growth, end of drought and recovery**

Gene ontology annotation and enrichment analysis was conducted to identify enriched GO terms associated with DAPs. The analysis was performed separately for proteins whose abundance increased or decreased under different conditions in the two genotypes, using the 7319 identified proteins as the background in Database for Annotation, Visualization, and Integrated Discovery (DAVID) (accessed in August 2025) [26]. Significantly enriched GO terms were selected based on ascending adjusted p-values, and the top 10 up and downregulated terms were selected.

Gene ontology analysis was conducted for biological processes (BPs), cellular components (CCs), and molecular functions (MFs). However, the presentation of results focuses primarily on the top enriched BPs (Figure 3), while related CCs and MFs are discussed only when necessary to avoid redundancy and maintain clarity. The top ten terms for BPs, CCs, and MFs, along with their GO IDs, number of proteins, fold enrichment, adjusted p-values, false discovery rate (FDR), and UniProt accessions, are provided in the Supplementary Tables (Supplementary Table S3-Table S5).

DAVID is a comprehensive and widely cited database that provides various functional annotation tools for both model and non-model species, although its coverage remains incomplete for some organisms. The recent versions of DAVID have been built upon the NCBI Entrez Gene system and the UniProt Knowledgebase [26]. Overall, GO analysis showed that a considerable number of DAPs could not be annotated in the two drought tolerant tef genotypes, and the number of GO terms exhibited relatively higher FDR values, reducing annotation bias and facilitating the discovery of novel processes associated with unannotated genes remain a challenge in enrichment analysis [27].

Carbohydrate metabolic processes were enriched among the DAPs with increased abundance under all conditions, except at the end of drought in Boni and during growth in RIL44. Response to heat, RNA splicing, L-proline biosynthetic process, and mRNA processing were among the most enriched BPs among DAPs with increased abundance in Boni at the end of drought and during early recovery. In addition, starch biosynthetic process was enriched in Boni at the end of drought and during late recovery. In contrast, in RIL44, the DAPs with increased abundance were mainly associated with cold acclimation, response to desiccation, and glyoxal metabolic processes at the end of drought. Hydrogen peroxide catabolic process was among BPs represented by DAPs with decreased abundance in both Boni and RIL44. However, this BP was enriched among DAPs with increased abundance during growth in Boni. In addition, response to oxidative stress was one of the most prominent BPs among DAPs with decreased abundance in Boni at the end of drought. However, it was enriched among DAPs with increased abundance during growth. Glucuronoxylan and chorismate were among the most prominent BPs represented by DAPs with decreased abundance in RIL44 at the end of drought, while glucuronoxylan BP was also downregulated during early recovery in Boni. In contrast, during early recovery xyloglucan metabolic process was enriched in Boni. Aromatic amino acid family BPs were downregulated in Boni at the end of drought and during recovery. Microtubule-based process and plant-type secondary cell wall biogenesis were the most prominent BPs among DAPs with decreased abundance at the end of drought and during early recovery in both Boni and RIL44; these BPs were also downregulated during early recovery in Boni and during growth in RIL44. During late recovery in Boni, the most enriched BPs were glycogen and starch BPs. In contrast, DAPs with decreased abundance during late recovery were mainly associated with methylation in both Boni and RIL44 and with lignan BP and vesicle budding from membrane in Boni.

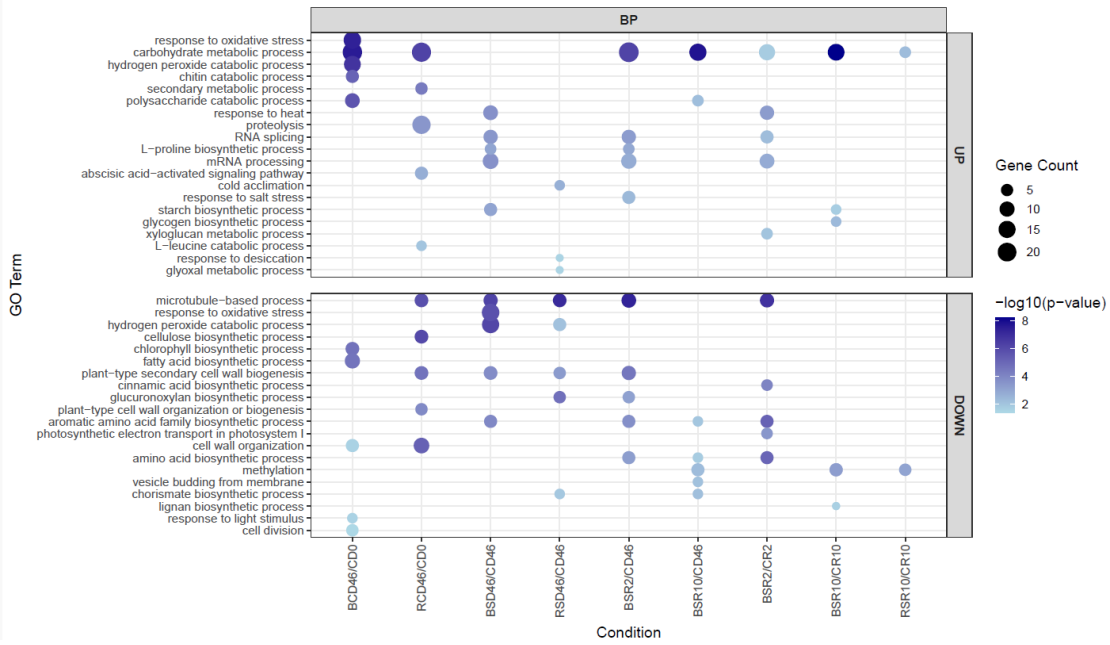


Figure 3 Top enriched biological processes (BPs) during growth, end of drought and recovery in two drought tolerant tef genotypes.

Note: The terms on the y-axis represent BPs, whereas the x-axis represents DAPs with paired treatment comparisons representing growth (CD46/CD0), the end of drought (SD46/CD46), and recovery (SR/CR). Where:BCD46/CD0: Boni control 46 days after drought stress vs control 0 days after drought stress, RCD46/CD0: RIL44 control after 46 of drought stress vs control 0 days after drought stress, BSD46/CD46: Boni stressed 46 days after drought stress vs control 46 days after drought stress, RSD46/CD46: RIL44 stressed 46 days after drought stress vs control 46 days after drought stress, BSR2/CD46: Boni drought stressed recovery after 2 days vs control 46 days after drought, BSR10/CD46: Boni stressed 10 days after drought stress vs control 46 days after drought, BSR2/CR2: Boni stressed 2 days after recovery vs control 2 days after recovery, BSR10/CR10: Boni drought stressed recovery after 10 days vs control after 10 days, and RSR10/CR10: RIL44 drought stressed after 10 days vs control after 10 days.

2.5 KEGG pathway analysis of DAPs with rice orthologs (*Oryza sativa* 'japonica group') during growth, end of drought and recovery

For further exploration of biological pathways, KEGG pathway analysis was done by converting tef DAPs from each conditions separately for proteins with increased and decreased abundance into their rice (*Oryza sativa japonica*) orthologs using g:Orth. Because the *E.tef* proteome is relatively under-annotated, resulting in limited KEGG and functional assignments, and although the *E. curvula* proteome provided broader protein sequence coverage for protein identification, its annotation was not sufficiently comprehensive for consistent KEGG pathway assignment. Therefore, the identified tef proteins were mapped to orthologous proteins in the highly annotated rice genome, enabling more reliable Ko assignment and subsequent KEGG pathway analysis [28]. Rice was selected as a reference because *E. tef* and *O. sativa* are both monocotyledonous grasses belonging to the family Poaceae.

The resulting orthologs were then analysed in g: GOSt to identify significantly enriched pathways ($p < 0.05$). The most enriched pathways were subsequently ranked based on ascending adjusted p-values. These results are presented in the Figure 4 below and table (Additional Table 2) at https://figshare.com/s/6e7dfb7f35c58ae1261e.

At the end of drought, biosynthesis of secondary metabolites was commonly represented among both upregulated and downregulated DAPs in Boni and RIL44. This pathway was also enriched among DAPs during growth and recovery stages. In Boni, starch and sucrose metabolism and arginine and proline

metabolism were highly represented among DAPs with increased abundance at the end of drought. In contrast, the biosynthesis of nucleotide sugars was represented by DAPs with decreased abundance in Boni at the end of drought and during early recovery. This pathway was also downregulated in RIL44 during growth. Moreover, phenylpropanoid biosynthesis was commonly represented among DAPs with decreased abundance in both genotypes at the end of drought and during early recovery.

During early recovery in Boni, amino acid biosynthesis and lysine degradation were the only pathways represented among DAPs with decreased and increased abundance, respectively, compared with the end of drought. During late recovery, amino sugar and nucleotide sugar metabolism, galactose metabolism and cyanoamino acid metabolism were additionally upregulated in Boni. Among the downregulated pathways, betalain biosynthesis was the only pathway that differed between late recovery and the end of drought in Boni. In addition, flavonoid biosynthesis was downregulated during late recovery which was also downregulated in RIL44 during growth.

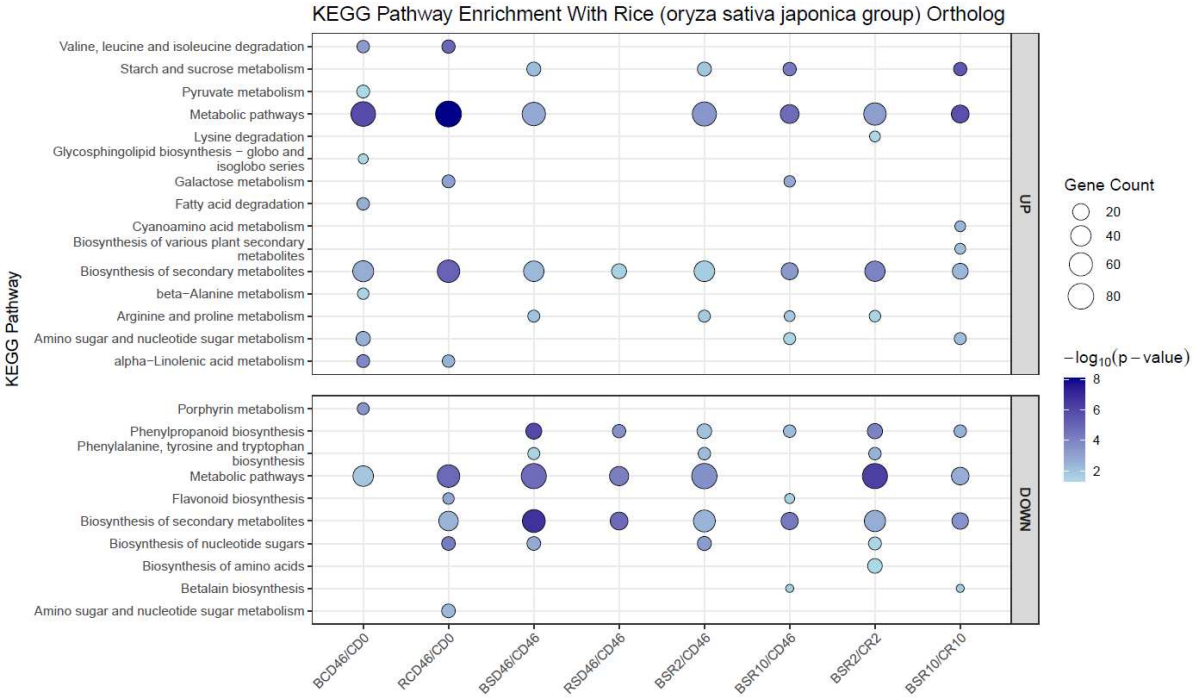


Figure 4 Top 10 enriched KEGG pathways identified from differentially abundant proteins (DAPs), converted to rice orthologs (oryza sativa japonica group), under growth, drought stress and recovery conditions.
Note: The terms on the y-axis represent KEGG pathways, whereas the x-axis represents DAPs with paired treatment comparisons representing growth (CD46/CD0), the end of drought (SD46/CD46), and recovery (SR/CR). Where: BCD46/CD0: Boni control 46 days after drought stress vs control 0 days after drought stress, RCD46/CD0: RIL44 control after 46 of drought stress vs control 0 days after drought stress, BSD46/CD46: Boni stressed 46 days after drought stress vs control 46 days after drought stress, RSD46/CD46: RIL44 stressed 46 days after drought stress vs control 46 days after drought stress, BSR2/CD46: Boni drought stressed recovery after 2 days vs control 46 days after drought, BSR10/CD46: Boni stressed 10 days after drought stress vs control 46 days after drought, BSR2/CR2: Boni stressed 2 days after recovery vs control 2 days after recovery, BSR10/CR10: Boni drought stressed recovery after 10 days vs control after 10 days, RSR10/CR10: RIL44 drought stressed after 10 days vs control after 10 days.

2.6 **Differential metabolite accumulation of two drought tolerant tef genotypes during growth, end of drought and recovery**

GC/MS analysis of metabolites in the two drought-tolerant tef genotypes identified 44 metabolites in total. After data pre-filtering and ANOVA, 31 significant metabolites were identified. These included 6 amino

acids, 10 sugars, 7 sugar alcohols, 6 organic and inorganic acids, and 2 unknown metabolites (Supplementary Table S6).

During the growth, ribose-1-phosphate was the only sugar that showed increased accumulation in Boni (Figure 5). In RIL44, the branched-chain amino acid (BCAA) isoleucine exhibited increased accumulation. Conversely, in Boni, the sugar alcohol glycerol showed decreased accumulation, while in RIL44, ribose showed reduced levels.

At the end of the drought, amino acids such as L-proline and glutamic acid, along with an unknown compound with a base peak of m/z 172 and a retention time of 9.48 minutes, showed increased accumulation in both genotypes. In addition, Boni exhibited an increased accumulation of sugar D-glucose. In RIL44, sucrose and sugar alcohols such as meso-erythritol and arabitol also showed increased accumulation.

In contrast, metabolites including isoleucine, fructose, glycerol, and succinic acid exhibited commonly decreased accumulation in both Boni and RIL44. Additionally, in Boni, sugars such as arabinose and lyxose, sorbitol, phosphoric acid, and an unknown compound (base peak of m/z 192 and a retention time of 10.20 minutes) showed reduced accumulation. In RIL44, the BCAAs leucine and valine, as well as ribose and lactic acid, also showed decreased accumulation.

During early recovery I, L-proline was the only amino acid that commonly increased in accumulation in both Boni and RIL44, consistent with its increased levels at the end of drought. In addition, Boni showed elevated levels of glutamic acid, meso-erythritol, and an unknown compound (base peak m/z 172, retention time 9.48 minutes). Both glutamic acid and the unknown compound also showed increased accumulation at the end of drought, while meso-erythritol appeared here for the first time in Boni but had already increased at the end of drought in RIL44. In RIL44, sucrose additionally showed increased accumulation, consistent with its increase at the end of drought.

Branched chain amino acids, including L-isoleucine and L-valine, showed decreased accumulation in both Boni and RIL44 during early recovery I. Isoleucine was reduced in both genotypes at the end of drought, whereas L-valine showed decreased accumulation only in RIL44 at that stage. In Boni, fructose, D-arabinose, and D-lyxose, succinic, citric acid, malic acids, the inorganic acid phosphoric acid, and an unknown compound (base peak m/z 192, retention time 10.20 minutes) all showed decreased accumulation. In RIL44, only lactic acid decreased in accumulation.

During early recovery II, L-proline again showed increased accumulation in both genotypes and remained the only commonly elevated metabolite. In Boni, arabitol was the only uniquely increased metabolite compared to early recovery I. Arabitol was first detected during early recovery in Boni, whereas it had already appeared earlier in RIL44 at the end of drought. The only metabolite that commonly decreased in both genotypes during early recovery II was malic acid.

In comparison with early recovery I, Boni showed decreased accumulation of myo-inositol, 4-guanidinobutyric acid, and lactic acid. The reduction in lactic acid first appeared during early recovery in Boni, while it was already observed in RIL44 both at the end of drought and during early recovery. In contrast, 4-guanidinobutyric acid and myo-inositol were newly observed as decreased metabolites at this stage only in Boni.

During late recovery I, arabitol showed increased accumulation in Boni, whereas the accumulation of sucrose and 4-guanidinobutyric acid increased in RIL44. Arabitol had previously shown increased accumulation at the end of drought in RIL44 and during early recovery in Boni. Sucrose consistently exhibited increased accumulation across all stages at the end of drought, early recovery, and late recovery in RIL44. In contrast, 4-guanidinobutyric acid decreased during early recovery in Boni but increased during late recovery in RIL44.

During late recovery II, meso-erythritol was the only metabolite that showed increased accumulation in Boni. This metabolite had also accumulated during early recovery in Boni and at the end of drought in RIL44. In RIL44, xylitol and succinic acid showed decreased accumulation during late recovery II. Xylitol was detected only during this stage, while succinic acid also showed decreased accumulation at the end of drought in both genotypes and during early recovery in Boni.

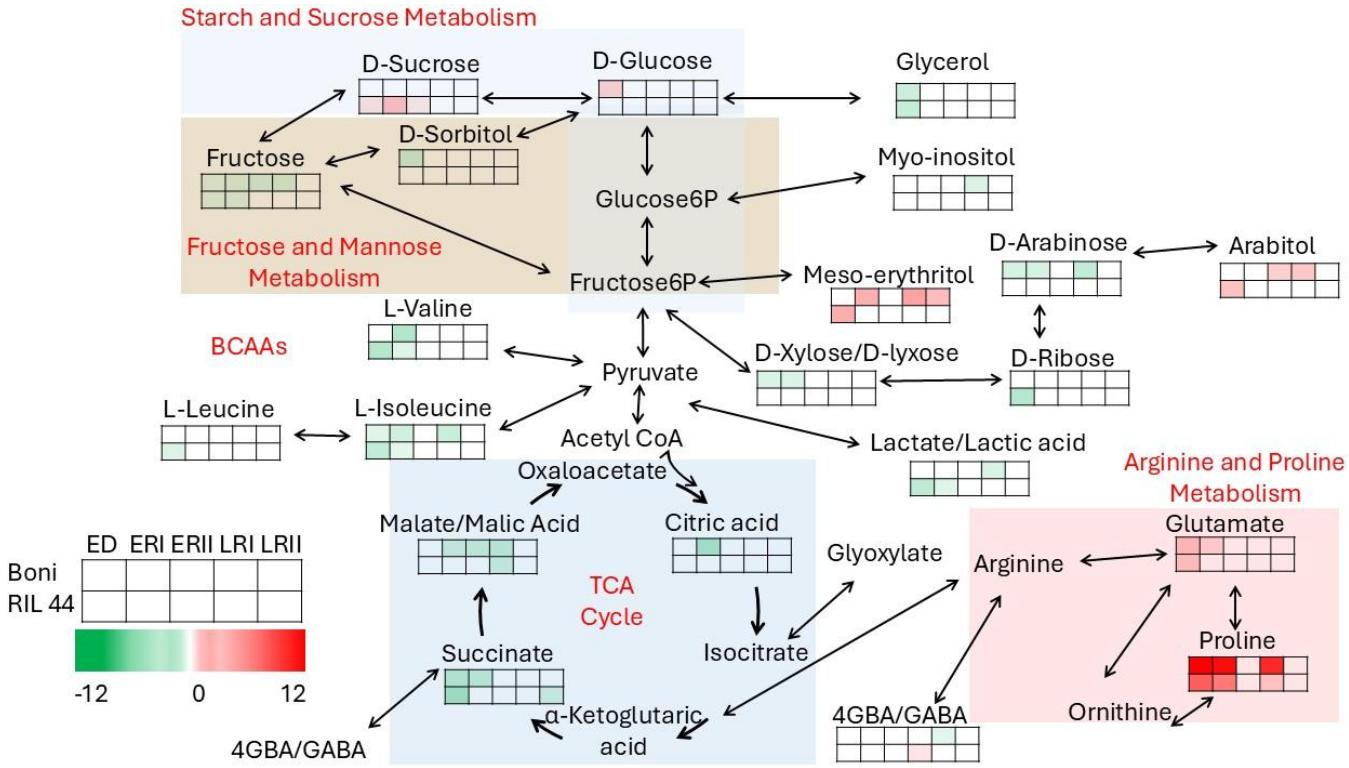


Figure 5 Metabolic network of the two drought tolerant tef genotypes at the end of drought, during early, and late recovery.

Where: ED: end of drought; ER: early recovery; LR: late recovery; BCAAs: branched chain amino acids, 4GBA: 4-guanidinobutyric acid; and GABA: Gama aminobutyric acid. **Note**: Colour intensity indicates the log-fold change of metabolites which showed significant ($P<0.05$) differential accumulation in drought stressed plants relative to their well-watered controls, where red represents increased accumulation and green represents decreased accumulation.

2.7 Comparison of selected proteins with metabolomic data during growth, drought, and recovery in two drought tolerant tef genotypes

Both the proteomic and metabolomic data presented in the previous sections revealed some enrichment of common pathways/processes during growth, at the end of drought and recovery (Table 2). In RIL44, valine, leucine, and isoleucine degradation pathways were enriched during growth. In contrast, Boni exhibited enrichment of arginine and proline metabolism, as well as starch and sucrose metabolism, specifically at the

end of drought. At the end of drought, RIL44 showed enrichment in secondary metabolite biosynthesis and glyoxal metabolic processes. During early recovery, Boni showed enrichment of arginine and proline metabolism.

Table 2 Comparison of selected proteins from the proteomic dataset with metabolomic data during growth, end of drought, and recovery in two drought-tolerant tef genotypes.

Conditions	Genotype	Metabolite	Protein	Accumulation /Abundance	KEGG Pathway
Growth	RIL44	Isoleucine	3-methyl-2-oxobutanoate dehydrogenase (2-methylpropanoyl-transferring) (EC 1.2.4.4) (Q0IPM2_ORYSJ)	Increased	Valine, leucine and isoleucine degradation
End of Drought	Boni	L-proline	Ornithine aminotransferase (EC 2.6.1.13) (OAT_ORYSJ)	Increased	Arginine and proline metabolism
		D-glucose	Glucose-1-phosphate adenylyltransferase large subunit 2, cytosolic (OsAGPL2) (OsAPL2) (EC 2.7.7.27) (A0A0P0VXA4_ORYSJ)	Increased	Starch and sucrose metabolism
		Glutamic acid	Ornithine aminotransferase, mitochondrial (EC 2.6.1.13) (OAT_ORYSJ)	Increased	Arginine and proline metabolism
	RIL44	L-proline	Delta-1-pyrroline-5-carboxylate synthase 2 (OsP5CS2) [Includes: Glutamate 5-kinase (GK) (EC 2.7.2.11) (P5CS2_ORYSJ)	Increased	Biosynthesis of secondary metabolites
		Glutamic acid	DJ-1/PfpI domain-containing protein (A0A5J9UI85)	Increased	
Early Recovery I	Boni	L-proline	Pyrroline-5-carboxylate reductase (EC 1.5.1.2) (A0A0P0VCR8_ORYSJ)	Increased	Arginine and proline metabolism
Early Recovery II	Boni	L-proline	Os05g0536400 protein (Os05g0536400 OSNPB_050536400)(B9FLB9_ORYSJ)	Increased	Arginine and proline metabolism

Note: Detailed information, including the corresponding GO terms (BP, CC, and MF), along with full protein descriptions, is available at the following link https://figshare.com/s/6e7dfb7f35c58ae1261e (Additional Table 3)

2.8 **Detailed KEGG Pathway analysis**

A global proteome comprising 7319 proteins was analysed using OmicsBox/Blast2GO to identify the associated KEGG pathways.

The identified pathways, together with the corresponding numbers of proteins, enzymes, and KEGG Orthologs (KOs), are summarized in Additional Table 4 and available at: https://figshare.com/s/6e7dfb7f35c58ae1261e. Based on the proteomic and metabolomic responses observed at the end of drought and during recovery, three biological pathways were selected for detailed analysis. The abundance patterns of proteins associated with enzymes within these pathways were examined to characterise their response to drought and recovery in the two drought tolerant tef genotypes.

Starch and sucrose metabolism

Starch and sucrose metabolism was associated with 182 proteins and 34 enzymes (Supplementary Figure S1 and Table S7). Consistent with previous studies, starch degradation and sugar remobilization may provide energy and osmolytes that enhance drought tolerance [29,30]. The increased abundance of glycogen phosphorylase (EC 2.4.1.1) indicated active starch degradation, while the simultaneous accumulation of glucose-1-phosphate adenylyltransferase (EC 2.7.7.27), starch synthase (EC:2.4.1.21), and 1,4-α-glucan branching (EC:2.4.1.18) enzyme, particularly in Boni, suggested continued starch biosynthesis and turnover. Glucose-6-phosphate appeared to be the primary precursor for starch synthesis, as alternative pathways were poorly represented. Enzymes involved in sucrose biosynthesis, including sucrose-phosphate synthase (SPS; EC:2.4.1.14) and sucrose-phosphate phosphatase (EC:3.1.3.24), also increased under drought, whereas sucrose synthase (EC:2.4.1.13) was relatively less abundant, indicating preferential sucrose synthesis through the SPS pathway. Increased abundance of sucrose and starch degrading enzymes further suggests enhanced glucose production to support osmotic adjustment, antioxidant defence, and stress signalling [31]. These proteomic results, together with the metabolomic evidence of glucose accumulation, indicate that drought-tolerant tef genotypes maintains a dynamic balance between starch turnover and soluble sugar production, enabling carbohydrate storage, osmoprotection, energy supply, and rapid metabolic recovery following rehydration.

Amino sugar and nucleotide sugar metabolism

This was represented by 121 proteins and 43 associated enzymes (Supplementary Figure S2 and Table S8). UDP-glucose, a central precursor for cell wall polysaccharides, was differentially allocated among pectin, xylan, arabinose, and glucose pathways. Although UDP-glucose 4-epimerase (EC:5.1.3.2) increased at the end of drought, the enzyme involved in pectin synthesis decreased, suggesting reduced pectin deposition at the end of drought. Similarly, enzymes involved in the synthesis of UDP-xylose and xylan showed lower abundance at the end of drought but increased during recovery, indicating suppression of secondary cell wall biosynthesis during dehydration and its restoration following rehydration. This is consistent with studies showing that reduced xylan and cellulose deposition increase cell wall flexibility, limits water loss, and enhances drought tolerance [32,33]. Arabinose metabolism followed a similar pattern, with reduced abundance during drought possibly reflecting its incorporation into flexible cell wall polymers or conversion to the osmoprotectant arabitol [34,35], as supported by the metabolomic analysis. Overall, these findings indicate that drought tolerant tef genotypes dynamically regulates cell wall metabolism by temporarily

reducing secondary cell wall biosynthesis while promoting soluble sugar production, thereby maintaining cell wall plasticity, enhancing stress tolerance, and facilitating recovery after rehydration.

Galactose metabolism

Galactinol is a central metabolite that can be converted into raffinose family oligosaccharides (RFOs) and can also feed into amino sugar, nucleotide sugar, and pentose phosphate metabolism (Supplementary Figure S3). *De novo* galactose synthesis occurs through nucleotide sugars via UDP-glucose 4-epimerase (EC:5.1.3.2), which showed no differential accumulation in either genotype at the end of drought. Galactose degradation through the Leloir pathway involves several enzymes (Supplementary Table S3), which were either absent or decreased at the end of drought.

UDP-Gal can be directed towards galactinol, RFOs, and sucrose biosynthesis. In both genotypes, enzymes within these pathways increased at the end of drought and generally declined during recovery, with stronger accumulation observed in Boni. Similar trends occurred for enzymes involved in manninotriose and melibiose metabolism. Raffinose and galactinol, contribute to drought tolerance through osmoprotection, antioxidant activity, and membrane stabilisation, and may provide energy during recovery [36,37].

Invertase, the enzyme responsible for catalysing sucrose to fructose showed no differential accumulation, consistent with decreased fructose levels in metabolomic dataset. In contrast, enzymes directing raffinose towards galactose and glucose increased during drought and recovery. Alpha-galactosidase (EC:3.2.1.22) which commonly catalyses galactose to galactinol, and other sugar alcohols also increased at the end of drought, despite decreased myo-inositol, sorbitol, and glycerol levels in the metabolomic data.

3 Discussion

3.1 **Differential abundance analysis of proteins**

Both Boni and RIL44 exhibited differential protein abundance across drought and recovery, although Boni consistently had more DAPs. It displayed the highest number of DAPs during early recovery, indicating extensive proteomic reprogramming following rehydration. On the other hand, RIL44 showed relatively few DAPs during recovery. This pattern agrees with the morphological changes, where RIL44 recovered more rapidly, as evidenced by earlier leaf unfolding (Figure 2). In contrast, the larger number of DAPs in Boni during early recovery likely reflects a slower recovery process requiring continued metabolic adjustment. Previous studies suggest that fewer DAPs or differentially expressed genes during recovery may represent an efficient drought-tolerance strategy by reducing energy expenditure on stress responses and redirecting resources toward growth and recovery [38,39].

3.2 **GO and KEGG pathway analysis**

The GO analysis resulted in the assignment of only a few DAPs. Functional annotation in non-model species remains challenging because only a limited number of genes were annotated [27,40]. Therefore, integrating GO and KEGG pathway analyses provides complementary insights by linking molecular pathways to changes in moisture conditions [41]. In addition, the GO annotation obtained from DAVID was supplemented by annotation of individual DAPs in the Uniprot knowledge database (accessed in August 2025) for identification of proteins/enzymes and related GO terms (https://www.uniprot.org/id-mapping).

Stress-responsive proteins and antioxidant mechanisms during drought and recovery

Gene ontology analysis revealed that drought induced the accumulation of stress-responsive proteins in both tef genotypes, including heat shock proteins (HSP70 and sHSPs), dehydrins, and late embryogenesis abundant (LEA) proteins. In Boni, increased proteins were associated with heat response (GO:0009408), whereas RIL44 showed enrichment for cold acclimation (GO:0009631) and desiccation response (GO:0009269). These proteins contribute to drought tolerance through protein stabilization, osmoprotection, ROS detoxification, and stress signalling [42–44]. HSP70 functions as a molecular chaperone by maintaining protein folding and preventing aggregation, while LEA proteins and dehydrins protect cellular components during dehydration and are strongly induced by ABA-dependent stress responses [43]. Similar increases in these proteins have been reported in drought-tolerant rice [45], salt tolerant transgenic tobacco, apple [46], and vegetative desiccation tolerant plants (also referred to as resurrection plants) [31,47], supporting their role as important components of drought adaptation.

In addition to stress proteins, Boni showed increased RNA processing and RNA splicing activity, dominated by RNA recognition motif (RRM) and CCCH zinc-finger proteins. These proteins may enhance stress tolerance by regulating post-transcriptional modification, alternative splicing, and stress-responsive gene expression [48,49]. Alternative splicing has been reported as an important mechanism in ABA-mediated drought responses [50,51] and has previously been observed in tef under water stress [8].

Antioxidant responses and metabolic adjustment

Despite the accumulation of stress proteins, GO analysis indicated reduced hydrogen peroxide catabolic activity in both genotypes and reduced oxidative stress response in Boni at the end of drought. This may reflect differences in antioxidant strategies. In RIL44, activation of glyoxal metabolism may contribute to oxidative protection by preventing toxic glyoxal accumulation [52,53], whereas Boni relied more on L-proline-associated antioxidant mechanisms. Proline functions as an osmoprotectant and ROS scavenger and has been linked with improved drought tolerance and maintenance of photosynthetic activity [54]. Increased ferritin abundance in both genotypes, particularly during recovery in Boni, may further protect cells by reducing iron-mediated oxidative damage [55,56]. Increased starch biosynthesis in Boni may also limit excessive soluble sugar accumulation could help to prevent oxidative stress and provide carbon reserves for recovery [53,57].

Shift in secondary metabolism during drought

Both genotypes showed reduced phenylpropanoid-related pathways, including aromatic amino acid and chorismate biosynthesis, suggesting reduced investment in phenolic and flavonoid production. Instead, increased abundance of tropinone reductase suggests a shift toward alkaloid biosynthesis. Since alkaloids can function as antioxidants and protective compounds [58,59], this transition may represent an alternative strategy for ROS management under severe drought stress.

Cell wall modification under drought and recovery conditions

Cell wall-related processes were among the major downregulated responses during drought. Both genotypes showed reduced microtubule-based processes and secondary cell wall biosynthesis, while RIL44 additionally showed reduced glucuronoxylan biosynthesis. These responses suggest suppression of cell wall thickening and expansion during severe dehydration, which may conserve carbon resources and maintain wall flexibility. Reduced cellulose, xylan, and lignin deposition can prevent excessive rigidity and facilitate recovery after rehydration [60]. This pattern agrees with previous studies showing that reduced secondary cell wall

formation can enhance drought tolerance by redirecting resources toward stress adaptation in sorghum [61,62] and resurrection grass species [63,64].

During recovery, Boni showed stronger activation of cell wall remodelling processes. Early recovery was characterized by increased abundance of FAS1 domain proteins, ABA receptor PYL8a, and xyloglucan endotransglucosylase/hydrolases. However, glucuronoxylan biosynthesis remained reduced, suggesting selective modification rather than complete restoration of secondary cell wall formation. Similar cell wall flexibility mechanisms have been reported in resurrection plants, where arabinose-rich polymers maintain wall plasticity and enable structural recovery after dehydration [64,67].

Recovery-associated metabolic changes in Boni

During early recovery, Boni showed increased lysine degradation and reduced amino acid biosynthesis pathways. Lysine degradation-associated aldehyde dehydrogenases may contribute to antioxidant defence by detoxifying reactive aldehydes produced during oxidative stress [68]. Reduced photosystem I activity during early recovery suggests that photosynthesis was not immediately restored, possibly preventing excess ROS production while cellular protection mechanisms remained active [69]. During late recovery, reduced methylation-related processes indicated a transition from stress responses toward normal growth and development [70].

Late recovery in Boni was characterized by increased amino sugar and nucleotide sugar metabolism, supporting cell wall reconstruction and growth through hemicellulose synthesis [71]. Increased β-glucosidase, β-galactosidase, and β-fucosidase activities further suggest active cell wall remodelling [72–74]. At the same time, reduced lignan biosynthesis and betalain pathways indicate decreased demand for secondary cell wall formation and antioxidant protection [75,76]. Reduced vesicle budding activity during recovery may also reflect a reduced requirement for stress-related protein transport and cellular defence mechanisms [77,78].

3.3 **Metabolic adjustments during drought stress and recovery**

Amino acid metabolism

Amino acid metabolism was strongly altered under drought stress, with increased accumulation of glutamic acid and proline in both Boni and RIL44 at the end of drought. The accumulation of these metabolites indicates enhanced osmotic adjustment, redox regulation, and stress protection [54,79]. Glutamate serves as a precursor for proline biosynthesis, and accumulated proline functions as a compatible solute that maintains cellular hydration, protects macromolecules, and scavenges ROS [80]. However, because proline accumulation had been reported in both drought-tolerant and susceptible plants, it may represent a general stress response rather than a specific biomarker of drought tolerance [81,82].

During recovery, proline remained elevated in both genotypes, although at lower levels than during drought, while glutamate persisted only in RIL44. The decline of these metabolites during recovery may indicate their utilization for energy production, nitrogen recycling, and restoration of growth [83]. Proline degradation provides reducing equivalents for mitochondrial respiration and generates glutamate, which can support nitrogen metabolism and amino acid synthesis during recovery [84]. This suggests that proline accumulation during drought and subsequent mobilization during recovery contribute to both stress protection and metabolic recovery.

In contrast, branched-chain amino acids (BCAAs) showed reduced accumulation, particularly in RIL44, while only isoleucine declined in Boni. Reduced BCAA levels may reflect their degradation to provide alternative respiratory substrates through pyruvate metabolism during drought-induced carbon limitation [85]. Similar reductions have been reported in drought-tolerant Arabidopsis mutants [86], sesame [87]mulberry [88], quinoa [89], and drought-tolerant tef genotypes [90]. Together with previous studies in tef and other plants, reduced isoleucine accumulation may represent a potential metabolic signature associated with drought adaptation [23]. During recovery, the increased accumulation of 4-guanidinobutyric acid in RIL44 suggests enhanced conversion of glutamate-derived metabolites, potentially supporting nitrogen metabolism, whereas the reduced level of this compound in Boni indicates a different glutamate utilization strategy [91].

Sugar and sugar alcohol metabolism

Soluble sugars showed genotype-specific accumulation patterns during drought. Glucose accumulated in Boni, whereas sucrose and meso-erythritol increased in RIL44. These metabolites contribute to drought adaptation through osmotic adjustment, energy supply, and signalling [92]. Sucrose and glucose are also involved in stress signalling pathways that regulate stomatal behaviour and adaptive responses [88]. The increased accumulation of meso-erythritol, together with reduced fructose levels, suggests enhanced carbon redistribution toward sugar alcohol production [93]. Sugar alcohols such as arabitol and meso-erythritol function as osmoprotectants and antioxidants by stabilizing membranes and protecting cellular components during dehydration [35].

Arabitol accumulation in RIL44 during drought suggests a role in both osmoprotection and cell wall adjustment, as arabinose-derived compounds contribute to arabinoxylan formation and maintenance of cell wall flexibility [64,94]. In contrast, reduced arabinose accumulation in Boni may indicate alternative utilization or delayed activation of this pathway, as arabitol increased during recovery. Reduced ribose, glycerol, and sorbitol levels in both genotypes may reflect their conversion into other carbohydrates or their preferential use for essential metabolic processes under severe drought [95,96]. The inconsistent responses of these metabolites across studies [31,95–97] indicate that individual sugars are unlikely to serve as universal drought tolerance biomarkers.

During recovery, Boni showed increased accumulation of meso-erythritol and arabitol. This is consistent with the proteomic results showing greater recovery-associated metabolic reprogramming in Boni compared with RIL44. These sugar alcohols may provide carbon reserves for rebuilding cellular structures while also protecting membranes and proteins during the transition from stress to growth [35,98,99]. The continued reduction of fructose and other sugars during recovery suggests their utilization for sucrose metabolism, cell wall restructuring, or energy production [60,100].

Organic and inorganic acid metabolism

Organic and inorganic acids generally declined during drought and recovery. Succinic acid, an intermediate of the TCA (tricarboxylic acid) cycle, decreased in RIL44, suggesting reduced respiratory activity under severe drought [101,102]. Similar reductions in TCA intermediates have been reported under drought stress, although responses vary among species and genotypes [87]. The reduction of phosphoric acid in Boni may reflect restricted phosphorus uptake or redistribution of phosphorus toward essential processes such as ATP synthesis, stress protein production, and osmolyte biosynthesis. Since phosphorus availability influences root

growth and drought adaptation, reduced shoot phosphoric acid may also indicate preferential allocation toward roots [103]. Tissue-specific metabolomic analysis would help clarify phosphorus partitioning in drought-tolerant tef.

During recovery, most organic and inorganic acids remained reduced, except for 4-guanidinobutyric acid. The reduced abundance of TCA intermediates suggests that respiratory metabolism was not immediately restored after rehydration [104], indicating a gradual transition from stress survival toward active growth.

3.4 **Comparison of proteomic and metabolomic responses**

Integration of proteomic and metabolomic datasets through shared KEGG pathways and biological processes provided complementary support of the molecular responses associated with drought tolerance in tef. Multi-omics approaches enable a more comprehensive understanding of stress regulation by linking changes in proteins, metabolites, and biochemical pathways, thereby improving interpretation of plant stress physiology and adaptation mechanisms [105–107]. In this study, arginine and proline metabolism was consistently enriched in both datasets, highlighting its central role in drought adaptation and recovery. Increased accumulation of proline and glutamic acid, together with proteomic evidence for enzymes such as ornithine aminotransferase and pyrroline-5-carboxylate synthase (P5CS2), supports enhanced production of osmoprotective metabolites that contribute to osmotic adjustment, antioxidant defence, and carbon and nitrogen recycling during recovery [54,84]. Similarly, starch and sucrose metabolism was enriched at the end of drought in both datasets, confirming its importance in providing soluble sugars for osmoprotection, energy supply, and carbon storage until photosynthetic activity is restored [108,109]. These results demonstrate that coordinated regulation of carbohydrate and amino acid metabolism represents a key mechanism underlying drought tolerance in tef.

4 Conclusion

This study revealed shared and genotype-specific molecular responses associated with dehydration and subsequent rehydration in two drought-tolerant tef genotypes. The proteomic and metabolomic findings suggest that drought tolerance involves changes in several biological processes, particularly those associated with cellular protection, osmotic adjustment, carbohydrate metabolism and cell wall modification. Under drought, both genotypes suppressed primary and secondary cell wall biosynthesis while redirecting carbon and nitrogen resources toward osmoprotective sugars, amino acids, and antioxidant pathways. Dynamic cell wall plasticity, carbohydrate remobilization, starch and sucrose metabolism, arginine–proline metabolism, and stress-responsive sugar pathways collectively enabled adaptation to severe dehydration and subsequent recovery. Upon rehydration, these processes were progressively reversed, promoting restoration of growth and metabolic homeostasis. Although both genotypes showed similar responses to dehydration, their responses during recovery differed. RIL44 showed faster initial recovery, whereas Boni exhibited greater restoration of leaf water content after 10 days, accompanied by more extensive changes in protein abundance during recovery. These findings suggest that the ability to withstand dehydration and recovery following rehydration may involve different molecular responses, highlighting the importance of considering both processes when evaluating drought resilience. The study also identified candidate proteins, metabolites and metabolic pathways that could be further investigated to better understand drought adaptation and support future crop improvement efforts.

5 Materials and Methods

Two drought tolerant tef genotypes with contrasting morphophysiological responses were used in this study. The genotypes were identified from two previous experiments conducted under dehydration alone [24] and dehydration–rehydration conditions [110] . Boni showed high-yielding capacity under dehydration conditions, whereas RIL44 showed early recovery after dehydration under rehydration conditions.

The pot experiment was conducted at the Forage Gene Bank of the International Livestock Research Institute (ILRI), Addis Ababa campus, Ethiopia. Addis Ababa is located at 9° 1′ 48″N latitude and 38° 44′ 24″E longitude, with an average elevation of approximately 2400 m above sea level. The mean annual temperatures ranging between 10.2 °C and 22.9 °C and an average annual rainfall of about 1150 mm [111].

5.1 **Experimental design**

The experiment was arranged in a completely randomized design (CRD) with two genotypes (Boni and RIL44) and two moisture conditions (drought-stressed and well-watered control), with five replicates each. Eight kg of soil was applied in each pot with 3:2:1 ratio of clay to vermicompost to sand. Fifty seeds were sown on each pot and thinned to 15 plants after three weeks. The plants were grown in a glasshouse (approximately 12 hrs light and 12hrs dark) with average day/night temperatures of 24.5 °C and 15.8 °C, and relative humidity levels of 71.2% and 94.5%, respectively.

Plants were subjected to drought stress at the booting stage. Booting (GS46) is the pre-flowering stage prior to panicle emergence [112]. Moisture stress at this stage critically determines flower fertility, which subsequently determines seed set, grain filling, and overall grain yield [113]. The control plants were maintained under well-watered conditions throughout the experiment. In contrast, drought-stressed plants were not irrigated from the booting stage for a total of 46 days. Following this period, the dehydrated plants were rehydrated to assess their recovery response. This level of stress was selected based on a previous experiment in which the plants were stressed until severe morphological changes were observed, as indicated by their leaf and soil moisture content [110].

5.2 **Sampling, storage and transport**

Approximately 4 cm of the tef stalk (culm) was sampled 1-2 cm above the soil surface, approximately between the first and second nodes of the tef stalk. This region is close to the crown, which is the origin of new tillers and emerging leaves [114], reflecting its high meristematic activity, particularly important during recovery. Moreover, sampling from the culm provides more consistent and reliable sampling location than leaves, as leaf tissues often exhibit variable phenotypes between dehydration and rehydration stages. Three tef plants were used for sampling from each pot as technical replicates. Samples were immediately wrapped in aluminium foil, flash-frozen in liquid nitrogen, and stored at -80 °C. Prior to transport, the samples were transferred to 5 mL Falcon tubes and freeze-dried at -48 °C for 48 hours. The freeze-dried samples were then transported and processed at the University of Cape Town, South Africa.

Samples were collected at four time points from all experimental units. Sampling was conducted at the beginning of drought (booting stage), at the end of drought (after 46 days of dehydration), and after 2 and 10 days of rehydration. At each sampling point, leaf relative water content (RWC) was determined gravimetrically for each sampled plant by taking the second leaf from the top, according to Willigen et al. [115]. Soil gravimetric water content (GWC) was also determined gravimetrically for each pot by collecting a soil sample at approximately 10 cm below the soil surface. The following formulas were used to calculate RWC and GWC:

$$GWC(\%) = \frac{fresh\ mass - dry\ mass}{dry\ mass} * 100$$

$$RWC(\%) = \frac{fresh\ mass - dry\ mass}{turgid\ mass - \ dry\ mass} * 100$$

5.3 **Protein extraction**

Approximately 1000 mg of tef stalk (culm) sample stored at -80°C was ground in liquid nitrogen using a chilled mortar and pestle. Protein extraction was conducted following the protocol described by Gabier et al. [31] with minor modifications. Briefly, 1 mL of cold TRIzol reagent (Sigma-Aldrich Corporation, St. Louis, MO, USA) was added to 100 mg of ground tissue and incubated for 5 minutes to allow dissociation of the nucleoprotein complex. Subsequently, 0.2 mL chloroform was added, the low protein binding Eppendorf tube was tightly closed, and the mixture was vortexed briefly. The sample was then incubated for 5 minutes and centrifuged at 12000 × g for 15 minutes at 4°C.

Following centrifugation, three distinct phases were formed. A lower red phenol-chloroform phase, an interphase, containing DNA and protein, and an upper colorless aqueous phase containing RNA. The upper phase was carefully removed by tilting the tube at a 45° angle, and 0.3 mL of 100% cold ethanol was added to the remaining interphase and organic phase. The tube was gently inverted several times to mix, incubated for 5 minutes, and then centrifuged at 2500 × g for 15 minutes at 4°C. The supernatant was transferred to a new tube containing 1.5 mL of isopropanol, incubated at room temperature for 5 minutes, and centrifuged again at 10250 × g for 15 minutes at 4°C.

The resulting supernatant was discarded, leaving the protein pellet at the bottom of the tube. The pellet was washed with 1mL of 0.1 M ammonium acetate in 100% methanol and centrifuged at 10250 × g for 5 minutes at 4°C. The supernatant was removed, and the pellet was further washed with 1mL of 100% acetone and centrifuged at 10250 × g for 2 minutes. Finally, the pellet was air-dried for 5 minutes and stored overnight at -80°C.

5.4 **Protein solubilization and quantification**

The protein pellet was solubilized in 100 µL of 500 mM triethylammonium bicarbonate (TEAB) containing 2% (w/v) SDS. The mixture was incubated at 95°C and vortexed five times, each for approximately five minutes, over a total period of ~1 hour until the pellet was completely dissolved. The homogenate was then centrifuged at 15700 × g for 10 minutes, and 95µL of the resulting supernatant was carefully collected. Protein concentration was determined using a bicinchoninic acid (BCA) assay kit according to the manufacturer's instructions (Sigma-Aldrich, USA, Cat. No. 23227).

5.5 **Hydrophilic interaction liquid chromatography (HILIC) on bead digest**

In preparation for the HILIC magnetic bead workflow, HILIC beads (ReSyn Biosciences, Cat. No. HLC010) were aliquoted into a new tube, and the shipping solution was carefully removed. The beads were washed twice with 250 µL of wash buffer (15% acetonitrile (ACN), 100 mM ammonium acetate, pH 4.5; Sigma, Cat. No. 14267) for 1 minute each. Subsequently, the beads were resuspended in loading buffer (30% ACN, 200 mM ammonium acetate, pH 4.5) to a final concentration of 2.5 mg mL^{-1}.

From each sample, 20µg of protein was transferred into a protein LoBind plate (Merck, Cat. No. 0030504.100). Proteins were reduced and alkylated by adding 20 mM dithiothreitol (DTT; Sigma, D9779)

and 30 mM iodoacetamide (IAA; Sigma, I6125) in equal volume to the sample, followed by incubation at 95°C for 10 minutes.

Following reduction and alkylation, HILIC magnetic beads were added to each sample at a 1:1 volume ratio and a 5:1 bead-to-protein ratio. The plate was then incubated at room temperature on a shaker at 900 rpm for 30 minutes to allow protein binding to the beads. After binding, the beads were washed four times with 500 µL of 95% ACN, each wash lasting 1 minute.

5.6 **Proteolytic digestion using trypsin and lysC**

For protein digestion, trypsin (Promega, Cat. No. PRV5111), prepared in 50 mM triethylammonium bicarbonate (TEAB), was added at a 1:20 ratio, and LysC (Pierce, Cat. No. 90307) was added at a 1:250 ratio. The plate was incubated at 45°C on a shaker for 2 hours to allow complete digestion. Following digestion, the supernatant containing the resulting peptides was carefully collected and dried under vacuum. The dried peptides were then resuspended in liquid chromatography (LC) loading buffer consisting of 0.1% formic acid (FA) and 2.5% acetonitrile (ACN).

5.7 **Liquid chromatography-tandem mass spectrometry (LC-MS/MS) analysis**

Liquid chromatography-mass spectrometry (LC-MS/MS) analysis was performed using a timsTOF Pro 2 mass spectrometer (Bruker, USA) with trapped ion mobility (TIMS) separation, coupled online via a Captivespray electrospray source (Bruker) to an Evosep One LC system (Evosep Biosystems, Denmark). Peptides were separated on a PepSep C18 column (150 µm × 8 cm, 1.5 µm; Bruker, Cat. No. 1893470) maintained at 40°C. Separation was achieved using a pre-formed linear gradient of solvents A (0.1% formic acid (FA) and B (100% acetonitrile (CAN) with 0.1% FA) over a 21-minute gradient (standard 60SPD Evosep One method).

The mass spectrometer was operated in positive ion mode. MS data were acquired using the "DIA PASEF-short gradient" method, with 25 Da mass windows, 21 mass steps per cycle, a 0.85-1.30 V·s/cm² CCS window, and a 100 ms TIMS accumulation window. Precursor ion scans were collected over m/z 100-1700, and fragment ion scans over m/z 475-1000. The estimated method duty cycle was 0.95s.

5.8 **Data processing and protein identification using Spectronaut**

Data analysis was performed using the tims (version 19.4.241104.62635, Biognosys AG). Protein identification was carried out against the *Eragrostis curvula* reference proteome database downloaded from UniProtKB (accessed in May 2025). All processing parameters were kept at their default settings, unless otherwise specified. *E. curvula* was used as the reference species for protein annotation because its UniProt reference proteome contains substantially more entries (53,659; Eragrostis curvula (weeping love grass) | Taxonomy) than that of *E. tef* (101 entries; Eragrostis tef (Teff) | Taxonomy). Furthermore, the *E. curvula* reference proteome has higher annotation scores than the available *E. tef* proteome.

The digestion enzymes were defined as trypsin/P and lysC/P. Variable modifications included N-terminal protein acetylation, deamidation of asparagine (N) and glutamine (Q), and oxidation of methionine (M), allowing a maximum of five variable modifications per peptide. A fixed modification of carbamidomethylation on cysteine residues (C), resulting from iodoacetamide alkylation (composition: C_2H_3NO; mass shift: +57.021464 Da), was also specified.

5.9 **Metabolites extraction**

The extraction and derivatization procedures were conducted according to Salem et al. [116], with some modifications. A total of 10 mg of homogenized sample was used after freeze-drying in a SpeedVac at 4°C (Savant SpeedVac SC100, Walter Fisher Scientific, Waltham, MA, USA) for 30 minutes.

One millilitre of pre-cooled (-20°C) extraction solvent (MTBE:MeOH, 3:1, v/v) containing ribitol at 0.1 mg mL^{-1} as an internal quantitative standard was added to a 2 mL screw-cap tube containing the homogenized sample. The mixture was vortexed for 30 seconds and incubated on an orbital shaker at 4°C for 30 minutes at 1000 rpm. Subsequently, the sample was sonicated in an ice-water bath for 15 minutes and centrifuged at 4°C for 5 minutes at 12000 rpm using a benchtop centrifuge.

The upper (green) phase (≈700 µL) was carefully transferred to a new tube, and 700 µL of pre-cooled H_2O:MeOH (3:1, v/v) was added. The mixture was vortexed for 10 seconds and centrifuged at 4°C for 5 minutes at 12000 rpm as before. The green upper layer was discarded, and 400 µL of the lower phase was carefully transferred to a fresh tube. All fractions were dried in a SpeedVac for approximately 5 hours and stored at -80°C until derivatization. A blank sample was also prepared in the same manner. Blank samples are used to trace and remove contaminants originating from the homogenized sample [117].

The remaining 300 µL of extract was used for quality control (QC) sample preparation. Pooled QC samples were prepared by combining 50 µL aliquots from each individual sample into a single tube. From this pooled mixture, three equal volumes (400 µL each) were prepared and used to run three separate analytical batches.

5.10 **Derivatization**

Before derivatization, the stored samples (-80°C) were freeze-dried in a SpeedVac for 30 minutes. Then, 40 µL of methoxyamine hydrochloride (MeOX; 20 mg mL^{-1} in pyridine) was added to the sample. The mixture was shaken on an orbital shaker at 1000 rpm for 2 hours at 37°C and then briefly centrifuged for 30 seconds. Subsequently, 70 µL of N-methyl-N-(trimethylsilyl) trifluoroacetamide (MSTFA) was added. The samples were shaken again at 37°C for 30 minutes and centrifuged for 2 minutes at 14000 rpm. Finally, 100 µL of the supernatant was transferred into glass GC vials with inserts for analysis. The blank sample was also derivatized using the same procedure. A library standards were used prepared in the same manner comprising amino acids (L-proline, L-leucine, L-valine, L-Isoleucine and gamma-aminobutyric acid), sugars (ribitol, D-glucose, D-fructose, D-sucrose, D-xylose, D-galactose and D-arabinose), sugar alcohol (glycerol, erythritol, D-mannitol, arabitol, myo-inositol, xylitol, D-sorbitol, D-thretitol), organic acids (lactic acid, malic acid, citric acid, succinic acid and quinic acid).

5.11 **GC/MS analysis**

Metabolite analysis was performed using an Agilent 7890A Gas Chromatograph coupled to an Agilent 7000C Triple Quadrupole Mass Spectrometer (Agilent Technologies, Santa Clara, CA, USA). Separation was achieved on an Agilent J&W DB-5Q column (30 m × 0.25 mm i.d., 0.25 µm film thickness) (Agilent, Germany) with constant ultrapure helium flow at 1 mL min^{-1}. Samples (1 µL) were injected using a 10 µL autosampler syringe with solvent A (0.1% formic acid) washes (4 cycles) before injection and solvent B (0.1% formic acid in acetonitrile) washes (4 cycles) afterward, along with two sample washes of 3 µL each and three sample pump cycles. Solvent and sample wash draw rates were 300 µL min^{-1} with dispense rates of 6000 µL min^{-1}, injection speed was 6000 µL min^{-1}, viscosity delay was 3 seconds, and an L1 air gap of 0.2 µL was applied. The injector operated in split mode (24:1), with inlet, transfer line, and ion source temperatures set at 240°C, 280°C, and 230°C, respectively, and electron-impact ionization at 70 eV. The GC

oven program started at 80°C (1 minute hold), ramped to 315°C at 8.5°C per minute, and held for 2 minutes, with a 7 minutes solvent delay and gas saver activated after 2 minutes. MS1 scan mode was applied over m/z 70–500 with a scan time of 208.8 ms per cycle (4.8 cycles/sec), a step size of 0.1 amu, threshold of 100, and gain factor of 1. Data acquisition and qualitative analysis were performed using Agilent MassHunter B.07.00, and quantitative analysis was conducted with Mass Hunter workstation software B.09.00 for GC/MS to acquire spectrum data for identifying known standards and internal standards.

5.12 **Identification, preparation of peak list and data preprocessing**

The spectral data were processed following the procedure described by Baluku et al. [118], involving peak resolution to identify metabolites present in the samples. Metabolite identification and quantification was carried out using the NIST08 MS library (National Institute of Standards and Technology, Gaithersburg, MD, USA) and by comparing retention indices with reference data. The sample containing the highest number of detected metabolites was selected to generate a master peak list, which was subsequently used to align the remaining samples, ensuring automatic peak alignment across all datasets. The processed results were exported, and quantification was performed by normalizing each metabolite's peak area against the internal ribitol standard.

5.13 **Statistical analysis**

Both proteomics and metabolite data were analysed using the MetaboAnalyst 6.0 online platform (R-based software; accessed August. 2025, https://www.metaboanalyst.ca/MetaboAnalyst/upload/StatUploadView.xhtml).

Proteins potentially representing contaminants with interquartile range less than 40% were removed. Also, metabolites potentially representing contaminants with an interquartile range of less than 5% were removed. Each treatment included five biological replicates, and proteins and metabolite features detected in less than 50% of the samples within a treatment were excluded. Missing values were imputed using one-fifth of the minimum positive value. Normalization and scaling were applied to minimize systematic variation and standardize the dataset [119]. Sample normalization was performed using the average peak area of internal standard (pooled quality control samples) to correct for technical variation [120]. Range scaling was then applied to protein features to approximate a near-normal distribution. Using range scaling, each value was transformed by subtracting the minimum and dividing by the variable's range [121]. For metabolites features, data were normalized using quantile normalization, followed by autoscaling to approximate a near-normal distribution.

A one-way ANOVA was performed to identify proteins and metabolites that differed significantly among the 16 treatments, using a significance threshold of $p < 0.05$ and FDR < 0.05 for multiple testing correction. The significantly different proteins and metabolites were subsequently used for differentially abundant and accumulation analysis between paired contrasting conditions within each genotype using Student's t-test. Proteins and Metabolites were considered significantly differentially abundant/accumulated when they exhibited a $\log_2$ fold change ($\log_2$FC) ±1, $p < 0.05$, and Benjamini–Hochberg-adjusted p-value (FDR) < 0.05.

5.14 **Gene ontology (GO) annotation**

Gene ontology annotation and enrichment analysis was conducted to identify biological pathways associated with the DAPs. The analysis was performed separately for increasingly abundant and diminished proteins from each condition and genotypes, using all identified proteins as the background reference.

Significantly enriched GO terms were identified by Fisher's exact test at a p-value < 0.05 and categorized into the three GO terms: biological process (BP), cellular component (CC), and molecular function (MF). The enriched GO terms were ranked by ascending p-values, and the top 10 upregulated and downregulated terms were retrieved. Additionally, the top 10 enriched BPs across the different conditions for both genotypes were visualized in a bubble plot using R version 4.3.3. Gene ontology identifiers (GO accession numbers) for individual DAPs were retrieved from UniProtKB (https://www.uniprot.org/id-mapping). Gene Ontology enrichment analysis was performed using DAVID 6.8 (Database for Annotation, Visualization and Integrated Discovery), a web-based bioinformatics tool designed for the functional annotation and enrichment of large gene and protein lists (accessed in August 2025) [26].

5.15 **KEGG pathway analysis**

The KEGG (Kyoto Encyclopedia of Genes and Genomes) pathway analysis was conducted separately for increasingly abundant and diminished DAPs from each condition. The UniProt accession IDs of tef DAPs were first converted to gene names in UniProt ID mapping tool. These gene names were then used to find rice (*Oryza sativa* japonica) orthologs through the g: Orth tool (https://biit.cs.ut.ee/gprofiler/orth). The resulting orthologs were subsequently analyzed using g: GOSt (https://biit.cs.ut.ee/gprofiler/gost) to determine significantly enriched KEGG pathways ($p < 0.05$) in an online bioinformatics tool g: Profiler. The top ten significantly enriched KEGG pathways were identified and visualized following the same procedure used for the GO analysis.

Pathway enrichment analysis was performed for the differentially accumulated metabolites (DAMs) using rice (*Oryza sativa* japonica) metabolomic data as the background in MetaboAnalyst 6.0. Furthermore, based on the pathway analysis output, the $\log_2$ fold change data, and information from KEGG (Kyoto Encyclopedia of Genes and Genomes) pathways, a metabolic network was constructed.

Finally, DAMs were identified separately for each condition and genotype, distinguishing between increased and decreased metabolites. The associated metabolic pathways were determined using pathway enrichment analysis in MetaboAnalyst, while the corresponding pathways for DAPs were identified through KEGG and GO analyses. The results were summarized in a table that integrates related metabolites and proteins, their accumulation patterns (increased/decreased), and the corresponding KEGG pathways and GO terms.

5.16 **Detailed KEGG pathway analysis**

The list of 7319 proteins with UniProt accession numbers was converted into FASTA format using the UniProtKB ID mapping tool (https://www.uniprot.org/id-mapping). The resulting FASTA file was imported into OmicsBox (version 3.6; accessed August 2025) for functional annotation. The analysis workflow included DIAMOND BLAST searches using default settings, InterProScan, GO mapping, GO annotation, EggNOG mapping and merging, EC number mapping, and combined pathway analysis for KEGG annotation with default setting.

The resulting KEGG pathway tables including the number of proteins, number of enzymes, KEGG Orthology (KO) identifiers, and corresponding enzymes and proteins were downloaded. Finally, based on the proteomic, metabolomic, and KEGG pathway analyses, key drought responsive pathways were identified and discussed.

Data Availability

The mass spectrometry proteomics data have been deposited to the ProteomeXchange Consortium via the PRIDE [1] partner repository with the dataset identifier PXD086999. The raw metabolomics data generated in this study are also publicly available at https://figshare.com/s/6e7dfb7f35c58ae1261e

References

1. Dai, A. Increasing drought under global warming in observations and models. *Nat. Clim. Chang.* **3**, 52–58 (2013).
2. Ming, A. *et al. Key Messages from the IPCC AR6 Climate Science Report*. (2021) doi:https://doi.org/10.33774/COE-2021-FJ53B.
3. Farrant, J. M. & Hilhorst, H. Crops for dry environments. *Curr. Opin. Biotechnol.* **74**, 84–91 (2022).
4. Tadele, Z. Orphan crops: their importance and the urgency of improvement. *Planta* vol. 250 677–694 Preprint at https://doi.org/10.1007/s00425-019-03210-6 (2019).
5. ESS. *Area and Production of Major Crops*. (2022).
6. Chanyalew, S. *et al.* Significance and prospects of an orphan crop tef. *Planta* **250**, 753–767 (2019).
7. Kebede, W. *et al.* Tef. in *Millets: Crops for climate resilience and for food and nutritional security* (eds. Piler, C. W., Shri, C. & Jain, M.) 271–302 (Springer Nature Singapore, 152 Beach Road, #21-01/04 Gateway East, Singapore 189721, Singapore, 2025). doi:https://doi.org/10.1007/978-981-95-1256-0_10.
8. Kamies, R., Farrant, J. M., Tadele, Z., Cannarozzi, G. & Rafudeen, M. S. A proteomic approach to investigate the drought response in the orphan crop Eragrostis tef. *Proteomes* **5**, 1–29 (2017).
9. Ali, M. S. Evaluating the response of teff [Eragrostis tef(Zucc.) Trotter] and hard red winter wheat (Triticum aestivum L.) to yield limiting factors in Oklahoma. (Oklahoma State University, Oklahoma, 2013).
10. Yihun, M. Y. Agricultural water productivity optimization for irrigated teff (Eragrostic Tef) in water scarce semi-arid region of Ethiopia. (Wageningen University, Delft, 2015).
11. Yumbya, John., Bij De Vaate, M. D., Kiambi, D., Kebebew, F. & Rao, K. *Assessing the Effects of Climate Change on Teff in Ethiopia : Implications for Food Security : Technical Report*. (African Biodiversity Conservation and Innovations Centre (ABCIC), Nairobi, Kenya, 2014).
12. Farooq, M., Wahid, A., Kobayashi, N., Fujita, D. & Basra, S. M. A. Plant drought stress: Effects, mechanisms and management. *Agronomy for Sustainable Development* vol. 29 185–212 Preprint at https://doi.org/10.1051/agro:2008021 (2009).
13. Fang, Y. & Xiong, L. General mechanisms of drought response and their application in drought resistance improvement in plants. *Cellular and Molecular Life Sciences* **72**, 673–689 (2015).
14. Xu, Z., Zhou, G. & Shimizu, H. Plant responses to drought and rewatering. *Plant Signal. Behav.* **5**, 649–654 (2010).
15. Khan, M. A. *et al.* Recent advances in molecular tool development for drought tolerance breeding in cereal crops: a review. *Zemdirbyste* **100**, 325–334 (2013).
16. Kumar, M., Patel, M. K., Kumar, N., Bajpai, A. B. & Siddique, K. H. M. Metabolomics and molecular approaches reveal drought stress tolerance in plants. *Int. J. Mol. Sci.* **22**, 1–23 (2021).
17. Nägele, T., Fürtauer, L., Nagler, M., Weiszmann, J. & Weckwerth, W. A strategy for functional interpretation of metabolomic time series data in context of metabolic network information. *Front. Mol. Biosci.* **3**, (2016).
18. Zenda, T. *et al.* Key maize drought-responsive genes and pathways revealed by comparative transcriptome and physiological analyses of contrasting inbred lines. *Int. J. Mol. Sci.* **20**, (2019).

19. Ghatak, A., Chaturvedi, P. & Weckwerth, W. Cereal crop proteomics: Systemic analysis of crop drought stress responses towards marker-assisted selection breeding. *Front. Plant Sci.* **8**, 1–25 (2017).

20. Saito, K. & Matsuda, F. Metabolomics for functional genomics, systems biology, and biotechnology. *Annu. Rev. Plant Biol.* **61**, 463–489 (2010).

21. Xu, Y. & Fu, X. Reprogramming of plant central metabolism in response to abiotic stresses: A metabolomics view. *Int. J. Mol. Sci.* **23**, 1–26 (2022).

22. Alemu, M. D. *et al.* Genomic dissection of productivity, lodging, and morpho-physiological traits in Eragrostis tef under contrasting water availabilities. *Plants People Planet* **7**, 1–19 (2024).

23. Girija, A. *et al.* Elucidating drought responsive networks in tef (Eragrostis tef) using phenomic and metabolomic approaches. *Physiol. Plant.* **174**, 1–12 (2022).

24. Girma, B. T., Roro, A. G., Abebe, K. A., Tadele, Z. & Farrant, J. M. The effect of drought on physiological and agronomic traits of tef [Eragrostis tef (Zucc.) Trotter]. *Front. Plant Sci.* **17**, 1–19 (2026).

25. Girma, B. T., Roro, A. G., Abebe, K. A., Tadele, Z. & Farrant, J. M. Physiological and Agronomic Responses of Tef (Eragrostis tef [Zucc.] Trotter) to Terminal Drought Stress. *Plants* **15**, 3588 (2026).

26. Sherman, B. T., Panzade, G., Imamichi, T. & Chang, W. DAVID Ortholog: an integrative tool to enhance functional analysis through orthologs. *Bioinformatics* **40**, 1–5 (2024).

27. Xue, B. & Rhee, S. Y. Status of genome function annotation in model organisms and crops. *Plant Direct* **7**, (2023).

28. Hamilton, J. P., Li, C. & Buell, C. R. The rice genome annotation project: An updated database for mining the rice genome. *Nucleic Acids Res.* **53**, D1614–D1622 (2025).

29. Smith, A. M. & Zeeman, S. C. Starch: A flexible, adaptable carbon store coupled to plant growth. *Annu. Rev. Plant Biol.* **16**, 217–245 (2020).

30. Thalmann, M. & Santelia, D. Starch as a determinant of plant fitness under abiotic stress. *New Phytologist* **214**, 943–951 (2017).

31. Gabier, H. *et al.* A label-free proteomic and complementary metabolomic analysis of leaves of the resurrection plant Xerophyta schlechteri during dehydration. . **11**, 1–24 (2021).

32. Coutinho, F. S. *et al.* Remodeling of the cell wall as a drought-tolerance mechanism of a soybean genotype revealed by global gene expression analysis. *aBIOTECH* **2**, 14–31 (2021).

33. Yan, J. *et al.* Increased drought tolerance in plants engineered for low lignin and low xylan content. *Biotechnol. Biofuels* **11**, 1–11 (2018).

34. Khan, M. S., Kanwal, B. & Nazir, S. Metabolic engineering of the chloroplast genome reveals that the yeast ArDH gene confers enhanced tolerance to salinity and drought in plants. *Front. Plant Sci.* **6**, 1–9 (2015).

35. Pamuru, R. R., Puli, C. O. R., Pandita, D. & Wani, S. H. Sugar alcohols and osmotic stress adaptation in plants. in *Compatible solutes engineering for crop plants facing climate change* (eds. Wani, S. H., Gangola, M. P. & Ramadoss, B. R.) 1–266 (Springer, Gewerbestrasse 11, 6330 Cham, Switzerland, 2021). doi:10.1007/978-3-030-80674-3.

36. Elsayed, A. I., Rafudeen, M. S. & Golldack, D. Physiological aspects of raffinose family oligosaccharides in plants: Protection against abiotic stress. *Plant Biol.* **16**, 1–8 (2014).

37. Yan, S., Liu, Q., Li, W., Yan, J. & Fernie, A. R. Raffinose Family Oligosaccharides: Crucial Regulators of Plant Development and Stress Responses. *CRC. Crit. Rev. Plant Sci.* **41**, 286–303 (2022).

38. Li, X. *et al.* Comparative proteomics analyses of intraspecific differences in the response of Stipa purpurea to drought. *Plant Divers.* **38**, 101–117 (2016).

39. Seneca, F. O. & Palumbi, S. R. The role of transcriptome resilience in resistance of corals to bleaching. *Mol. Ecol.* **24**, 1467–1484 (2015).

40. Gabier, H. Label-free proteomic analysis of Xerophyta schlechteri leaf tissue under dehydration stress. (University of Cape Town, Cape Town, 2020).

41. Ali, A. E. E., Husselmann, L. H., Tabb, D. L. & Ludidi, N. Comparative proteomics analysis between maize and sorghum uncovers important proteins and metabolic pathways mediating drought tolerance. . **13**, 1–15 (2023).

42. Sun, Z. *et al.* Molecular sciences plant dehydrins: Expression, regulatory networks, and protective roles in plants challenged by abiotic stress. *J. Mol. Sci* **22**, 1–17 (2021).

43. Artur, M. A. S. *et al.* Structural plasticity of intrinsically disordered LEA proteins from Xerophyta schlechteri provides protection in vitro and in vivo. *Front. Plant Sci.* **10**, (2019).

44. Olvera-Carrillo, Y., Campos, F., Reyes, J. L., Garciarrubio, A. & Covarrubias, A. A. Functional analysis of the group 4 late embryogenesis abundant proteins reveals their relevance in the adaptive response during water deficit in arabidopsis. *Plant Physiol.* **154**, 373–390 (2011).

45. Kou, S. Y. *et al.* Heterologous expression of heat-shock protein PpHSP70 improves high temperature and drought tolerance in rice. *Plant Stress* **10**, 1–6 (2023).

46. Han, X. *et al.* Systematic identification and analysis of the HSP70 genes reveals MdHSP70-38 enhanced salt tolerance in transgenic tobacco and apple. *Int. J. Biol. Macromol.* **289**, 1–12 (2025).

47. Pardo, J. *et al.* Intertwined signatures of desiccation and drought tolerance in grasses. *Proc. Natl. Acad. Sci. U. S. A.* **117**, 10079–10088 (2020).

48. Grimaldi, G. *et al.* PARPs and PAR as novel pharmacological targets for the treatment of stress granule-associated disorders. *Biochem. Pharmacol.* **167**, 64–75 (2019).

49. Han, G., Qiao, Z., Li, Y., Wang, C. & Wang, B. The roles of ccch zinc-finger proteins in plant abiotic stress tolerance. *Int. J. Mol. Sci.* **22**, 1–20 (2021).

50. Hamzelou, S. Proteomics of rice in response to drought stress. (Macquarie University, Sydney, New South Wales, Australia, 2021).

51. Laloum, T., Martín, G. & Duque, P. Alternative splicing control of abiotic stress responses. *Trends Plant Sci.* **23**, 140–150 (2018).

52. Hoque, T. S. *et al.* Methylglyoxal: An emerging signaling molecule in plant abiotic stress responses and tolerance. *Front. Plant Sci.* **7**, 1–11 (2016).

53. Mostofa, M. G. *et al.* Methylglyoxal – a signaling molecule in plant abiotic stress responses. *Free Radic. Biol. Med.* **122**, 96–109 (2018).

54. Meena, M. *et al.* Regulation of L-proline biosynthesis, signal transduction, transport, accumulation and its vital role in plants during variable environmental conditions. *Heliyon* **5**, 1–20 (2019).

55. Kabir, A. H. *et al.* Transcriptional shifts and microbiome dynamics in sorghum roots during vegetative growth under drought stress. **Pre-print**, (2024).

56. Ravet, K. *et al.* Ferritins control interaction between iron homeostasis and oxidative stress in Arabidopsis. *Plant Journal* **57**, 400–412 (2009).

57. Paudel, G. *et al.* Osmotic stress is accompanied by protein glycation in Arabidopsis thaliana. *J. Exp. Bot.* **67**, 6283–6295 (2016).

58. Gutiérrez-Grijalva, E. P., López-Martínez, L. X., Contreras-Angulo, L. A., Elizalde-Romero, C. A. & Heredia, J. B. Plant alkaloids: Structures and bioactive properties. in *Plant-derived bioactives: Chemistry and mode of action* (ed. Swamy, M. K.) 85–117 (Springer Singapore, Singapore, 2020). doi:10.1007/978-981-15-2361-8_5.

59. Yoo, Y. *et al.* Caffeine produced in rice plants provides tolerance to water-deficit stress. *Antioxidants* **12**, 1 (2023).

60. Le Gall, H. *et al.* Cell wall metabolism in response to abiotic stress. *Plants* **4**, 112–166 (2015).

61. Ali, E. A. E. Comparative molecular, physiological and proteomic analyses of maize and sorghum subjected to water deficit stress. (University of the Western Cape, Cape Town, 2019).

62. Goche, T. *et al.* Comparative physiological and root proteome analyses of two sorghum varieties responding to water limitation. *Sci. Rep.* **10**, 1–18 (2020).

63. Moore, J. P., Vicré-Gibouin, M., Farrant, J. M. & Driouich, A. Adaptations of higher plant cell walls to water loss: Drought vs desiccation. *Physiol. Plant.* **134**, 237–245 (2008).

64. Moore, J. P., Vicré, M., Nguema-Ona, E., Driouich, A. & Farrant, J. M. Drying out walls: How do the cell walls of resurrection plants survive desiccation? in *Plant Cell Walls: Research Milestones and Conceptual Insights* (ed. Geitmann, A.) 441–451 (CRC Press, 2023). doi:10.1201/9781003178309-22.

65. Plancot, B. *et al.* Structural characterization of arabinoxylans from two African plant species Eragrostis nindensis and Eragrostis tef using various mass spectrometric methods. *Rapid Communications in Mass Spectrometry* **28**, 908–916 (2014).

66. Zhao, J., Missihoun, T. D. & Bartels, D. The role of Arabidopsis aldehyde dehydrogenase genes in response to high temperature and stress combinations. *J. Exp. Bot.* **68**, 4295–4308 (2017).

67. Zivcak, M. *et al.* Photosynthetic electron transport and specific photoprotective responses in wheat leaves under drought stress. *Photosynth. Res.* **117**, 529–546 (2013).

68. Rao, X., Yang, S., Lü, S. & Yang, P. DNA methylation dynamics in response to drought stress in crops. *Plants* **13**, 1–18 (2024).

69. Zhang, W., Qin, W., Li, H. & Wu, A. M. Biosynthesis and transport of nucleotide sugars for plant hemicellulose. *Front. Plant Sci.* **12**, 1–13 (2021).

70. Cairns, K. J. R., Karunambigai, A., Jeon, J. S. & Svasti, J. Functions of rice beta-glucosidases and transglucosidases. *ScienceAsia* **49**, 635–645 (2023).

71. Chandrasekar, B. & Van Der Hoorn, R. A. L. Beta galactosidases in Arabidopsis and tomato - A mini review. *Biochem. Soc. Trans.* **44**, 150–158 (2016).

72. Günl, M. *et al.* AXY8 encodes an α-fucosidase, underscoring the importance of apoplastic metabolism on the fine structure of Arabidopsis cell wall polysaccharides. *Plant Cell* **23**, 4025–4040 (2011).

73. Timoneda, A. *et al.* The evolution of betalain biosynthesis in Caryophyllales. *New Phytologist* **224**, 71–85 (2019).

74. Choi, S. J., Lee, Z., Kim, S., Jeong, E. & Shim, J. S. Modulation of lignin biosynthesis for drought tolerance in plants. *Front. Plant Sci.* **14**, 1–14 (2023).

75. Bonifacino, J. S. & Glick, B. S. The mechanisms of vesicle Budding and fusion. *Cell* **116**, 153–166 (2004).

76. Tripathy, M. K., Deswal, R. & Sopory, S. K. Plant RABs: Role in development and in abiotic and biotic stress responses. *Curr. Genomics* **22**, 26–40 (2021).

77. Bowne, J. B. *et al.* Drought responses of leaf tissues from wheat cultivars of differing drought tolerance at the metabolite level. *Mol. Plant* **5**, 418–429 (2012).

78. Verslues, P. E. & Sharma, S. Proline Metabolism and Its Implications for Plant-Environment Interaction. *Arabidopsis Book* **8**, 1–23 (2010).

79. Lv, L. *et al.* Different adaptive patterns of wheat with different drought tolerance under drought stresses and rehydration revealed by integrated metabolomic and transcriptomic analysis. *Front. Plant Sci.* **13**, 1–17 (2022).

80. Nam, K. H. *et al.* Metabolomic changes in grains of well-watered and drought-stressed transgenic rice. *J. Sci. Food Agric.* **96**, 807–814 (2016).

81. Szabados, L. & Savouré, A. Proline: a multifunctional amino acid. *Trends Plant Sci.* **15**, 89–97 (2010).

82. Kishor, P. B. K. & Sreenivasulu, N. Is proline accumulation per se correlated with stress tolerance or is proline homeostasis a more critical issue? *Plant Cell Environ.* **37**, 300–311 (2014).

83. Ingrisano, R., Tosato, E., Trost, P., Gurrieri, L. & Sparla, F. Proline, cysteine and branched-chain amino acids in abiotic stress response of land plants and microalgae. *Plants* **12**, 1–15 (2023).

84. Pires, M. V. *et al.* The influence of alternative pathways of respiration that utilize branched-chain amino acids following water shortage in Arabidopsis. *Plant Cell Environ.* **39**, 1304–1319 (2016).

85. You, J. *et al.* Transcriptomic and metabolomic profiling of drought-tolerant and susceptible sesame genotypes in response to drought stress. *BMC Plant Biol.* **19**, 1–16 (2019).

86. Ackah, M. *et al.* Metabolomics response to drought stress in Morus alba L. Variety Yu-711. *Plants* **10**, 1–35 (2021).

87. Zhu, X. *et al.* Non-targeted metabolomics analysis of metabolite changes in two quinoa genotypes under drought stress. *BMC Plant Biol.* **23**, (2023).

88. Girija, A., Yadav, R., Corke, F., Doonan, J. & Mur, L. A. J. Untargeted metabolomic profiling reveals variation in metabolites associated with nutritional values in tef accessions. *Plant Foods for Human Nutrition* **76**, 536–539 (2021).

89. Forde, B. G. & Lea, P. J. Glutamate in plants: Metabolism, regulation, and signalling. *J. Exp. Bot.* **58**, 2339–2358 (2007).

90. Rosa, M. *et al.* Soluble sugars—metabolism, sensing and abiotic stress. *Landes Bioscience* **4**, 388–393 (2009).

91. Hilal, M. *et al.* Epidermal lignin deposition in quinoa cotyledons in response to UV-B radiation. *Photochem. Photobiol.* **79**, 1–17 (2004).

92. Tenhaken, R. Cell wall remodeling under abiotic stress. *Front. Plant Sci.* **5**, 1–9 (2015).

93. Conde, A. *et al.* Polyols in grape berry: Transport and metabolic adjustments as a physiological strategy for water-deficit stress tolerance in grapevine. *J. Exp. Bot.* **66**, 889–906 (2014).

94. Foti, C., Kalampokis, I. F., Aliferis, K. A. & Pavli, O. I. Metabolic responses of two contrasting lentil genotypes to peg-induced drought stress. *Agronomy* **11**, 1–18 (2021).

95. Eastmond, P. J. Glycerol-insensitive Arabidopsis mutants: gli1 seedlings lack glycerol kinase, accumulate glycerol and are more resistant to abiotic stress. *Plant Journal* **37**, 617–625 (2004).

96. Hassan, M. J. *et al.* Diethyl aminoethyl hexanoate reprogramed accumulations of organic metabolites associated with water balance and metabolic homeostasis in white clover under drought stress. *Front. Plant Sci.* **15**, 1–14 (2024).

97. Nahar, K., Hasanuzzaman, M. & Fujita, M. Roles of osmolytes in plant adaptation to drought and salinity. in *Osmolytes and Plants Acclimation to Changing Environment: Emerging Omics Technologies* (eds. Iqbal, N., Khan, N. A. & Nazar, R.) 37–68 (Springer India, New Delhi, India, 2016). doi:10.1007/978-81-322-2616-1_4.

98. Kordowska-Wiater, M. Production of arabitol by yeasts: Current status and future prospects. *J. Appl. Microbiol.* **119**, 303–314 (2015).

99. Du, H., Wang, Z., Yu, W. & Huang, B. Metabolic responses of hybrid bermudagrass to short-term and long-term drought stress. *J. Amer. Soc. Hort. Sci* **137**, 411–420 (2012).

100. Pavli, O. I., Vlachos, C. E., Kalloniati, C., Flemetakis, E. & Skaracis, G. N. Metabolite profiling reveals the effect of drought on sorghum (Sorghum bicolor L. Moench) metabolism. *POJ* **6**, 371–376 (2013).

101. Kandhol, N. *et al.* Link between plant phosphate and drought stress responses. *Research* **7**, 1–4 (2024).

102. Zhang, Y. & Fernie, A. R. The Role of TCA Cycle Enzymes in Plants. *Adv. Biol.* **7**, 1–12 (2023).

103. Hao, Y., Zhang, Z., Luo, E., Yang, J. & Wang, S. Plant metabolomics: Applications and challenges in the era of multi-omics big data. *aBIOTECH* **6**, 116–132 (2025).

104. Ma, X. *et al.* Integrated transcriptomic, proteomic and metabolomic analyses revealing the roles of amino acid and sucrose metabolism in augmenting drought tolerance in Agropyron mongolicum. *Front. Plant Sci.* **15**, 1–19 (2024).

105. Wang, Y., Tong, L., Liu, H., Li, B. & Zhang, R. Integrated metabolome and transcriptome analysis of maize roots response to different degrees of drought stress. *BMC Plant Biol.* **25**, 1–17 (2025).

106. Rosa, M. *et al.* Soluble sugars-Metabolism, sensing and abiotic stress. *Plant Signal. Behav.* **4**, 388–393 (2009).

107. AbdElgawad, H. *et al.* Starch biosynthesis contributes to the maintenance of photosynthesis and leaf growth under drought stress in maize. *Plant Cell Environ.* **43**, 2254–2271 (2020).

108. Girma, B. T., Roro, A. G., Abebe, K. A., Tadele, Z. & Farrant, J. M. Physiological and Agronomic Responses of Tef (Eragrostis tef [Zucc.] Trotter) to Terminal Drought Stress. *Pre-print* 1–20 (2026) doi:10.20944/preprints202609.1952.v1.

109. Mekonnen, E. N., Fetene, A. & Gebremariam, E. Grid-based climate variability analysis of Addis Ababa, Ethiopia. *Heliyon* **10**, 1–30 (2024).

110. Tottman, D. R. & Brod, H. The decimal code for the growth stages of cereals, with illustrations. *Ann. appl. Biol* **110**, 441–454 (1987).

111. Qiao, M., Hong, C., Jiao, Y., Hou, S. & Gao, H. Impacts of drought on photosynthesis in major food crops and the related mechanisms of plant responses to drought. *Plants* **13**, 1–19 (2024).

112. Shaaf, S., Bretani, G., Biswas, A., Fontana, I. M. & Rossini, L. Genetics of barley tiller and leaf development. *J. Integr. Plant Biol.* **61**, 226–256 (2019).

113. Willigen, C. Vander, Pammenter, N. W., Mundree, S. & Farrant, J. Some physiological comparisons between the resurrection grass, Eragrostis nindensis, and the related desiccation-sensitive species, E. curvula. *Plant Growth Regul.* **35**, 121–129 (2001).

114. Salem, M. A. *et al.* An improved extraction method enables the comprehensive analysis of lipids, proteins, metabolites and phytohormones from a single sample of leaf tissue under water-deficit stress. *Plant Journal* **103**, 1614–1632 (2020).

115. Gupta, P., Dhanya, A. J., Sharma, R. & Sreelakshmi, Y. Identification of Volatiles in Tomato Fruit Using Headspace Solid-Phase-Micro-Extraction (HS-SPME) Coupled with Gas Chromatography-Mass Spectrometry (GC-MS). in *Plant functional genomics: Methods and protocols* (ed. Maghuly, F.) vol. 2788 39–48 (Humana Press, New York, New York, NY 10004, U.S.A., 2024).

116. Baluku, E., Van Der Pas, L., Hilhorst, H. W. & Farrant, J. M. Metabolite profiling of the resurrection grass Eragrostis nindensis during desiccation and recovery. *Plants* **13**, 1–18 (2025).

117. Xia, J., Mandal, R., Sinelnikov, I. V., Broadhurst, D. & Wishart, D. S. MetaboAnalyst 2.0-a comprehensive server for metabolomic data analysis. *Nucleic Acids Res.* **40**, 127–133 (2012).

118. O'rourke, M. B. *et al.* What is normalization? The strategies employed in top-down and bottom-up proteome analysis workflows. *Proteomes* **7**, 1–19 (2019).

119. Pang, Z. *et al.* MetaboAnalyst 6.0: towards a unified platform for metabolomics data processing, analysis and interpretation. *Nucleic Acids Res.* **52**, 398–406 (2024).

Acknowledgments

We acknowledge the Department of Molecular and Cell Biology at the University of Cape Town for providing access to the GC/MS facility. We are especially grateful to Ms. Pei-Yin Liebrich for her assistance with metabolite analysis and to the D-CYPHR team for conducting the proteomic analyses. We extend our sincere thanks to Mr. Alemayehu Demeke, Mr. Tekele Hundesa, Mr. Assefa Bezie and Ms. Bersabe Solomon at the International Livestock Research Institute (ILRI), Addis Ababa Campus, for their assistance with the glasshouse experiment and for providing support to the −80°C freezer for sample storage. We also gratefully acknowledge Dr. Chris Jones of ILRI for providing access to these facilities. We sincerely acknowledge Mr. Tamiru Olbana, Dr. Driba Geleti, Mr. Million, Freight in Time Logistics, Ms. Keren Cooper, and Mr. Ali Kiyaei for facilitating the import and export of the samples. Finally, EIAR gratefully acknowledged for granting long-term study leave to the first author.

Author Contributions

The study was conceptualized by JMF, ZT, AGR, and KAA and all research and analysis were done be BTG. LVP and HG guided the data analysis. BTG generated the original manuscript, which all authors except KAA edited.

Additional Information

Competing Interests

The authors declare that the research was conducted in the absence of any commercial or financial relationships that could be construed as a potential conflict of interest.

Funding

This work was supported by the NRF SARChI research grant (grant No. 98406). The PhD study of the first author was funded by the NRF Postgraduate Scholarship (grant No. MND210427597691/ PMDS240524220660-PR-2025).